Public Policy Research Funding Scheme

公共政策研究資助計劃

Project Number : 項目編號：	2021.A6.184.21D
Project Title : 項目名稱：	Identifying and Prioritizing Development Zones for Green Roofs in Hong Kong: A Geospatial Smart City Way towards Carbon Neutrality 香港綠色屋頂發展區域的潛力識別和優先級排序：通向碳中和的地理空間智慧城市之路
Principal Investigator : 首席研究員：	Dr YAO Wei 姚巍博士
Institution/Think Tank : 院校 ／智庫：	The Hong Kong Polytechnic University 香港理工大學
Project Duration (Month): 推行期 (月) ：	15
Funding (HK$) : 總金額 (HK$)：	599,150.00

Identifying and Prioritizing Development Zones for Green Roofs in Hong Kong: A Geospatial Smart City Way towards Carbon Neutrality

香港綠色屋頂發展區域的潛力識別和優先級排序：通向碳中和的地理空間智慧城市之路

Final Report

Prepared by

Wei Yao, Department of Land Surveying & Geo-Informatics, The Hong Kong Polytechnic University

John Shi, Department of Land Surveying & Geo-Informatics, The Hong Kong Polytechnic University

Charles Wong, Department of Land Surveying & Geo-Informatics, The Hong Kong Polytechnic University

15.08.2023

Acknowledgement

This research project (Project Number: 2021.A6.184.21D) is funded by the Public Policy Research Funding Scheme of The Government of the Hong Kong Special Administrative Region.

Table of Contents

Executive Summary (in both English and Chinese languages)

1) Abstract of the Research

Hong Kong is a highly dense city and has experienced increased pressure on social, economic, and environmental sectors due to the rapid urbanization and increasing risk posed by climate change. The greenhouse gas emission incurred by population development have increased to an unprecedented high level, being a major contributing factor to global warming. The mitigation of climate change toward a livable and sustainable city became a major public consensus. To encourage the usage of low-carbon facility and technology in Hong Kong, solutions such as green roofs (GRs) are often put forward in the context of smart and sustainable city as they present a multi-functional and solution-oriented approach to address current challenges. Green roofs are of extreme relevance to highly compact cities with abundant impervious surfaces. GRs not only provide extra green spaces but also improve cityscape and attenuate urban heat island effect. Buildings with large sized roofs are usually owned by government or commercial agencies, making those buildings more relevant to green roofs retrofitting. Since 2001 HK government incorporated roof greening designs into new government building projects, while retrofitted roof greening is introduced to the roof works of existing buildings.

This project aims at utilizing a well-established smart city platform for Hong Kong geospatial data infrastructure including land use map, 3D building model/cadaster, ancillary tertiary planning data, satellite images and airborne LiDAR data to determine available rooftop areas to accommodate GRs system, and to quantify total benefits of deployment to Hong Kong. We identify the potential locations of GRs at a city scale using parameters such as planarity, area and slope of the rooftop as well as construction structure of buildings. The development zones are prioritized based on environmental, transportation, building attributes, ecological and socio-economic factors, as the implementation of GRs is of high priority but might be unaffordable for the residents in socio-economic deprivation zones. Upon completion of the project, it suggests the potential utilization rate of rooftops of more than 312,170 buildings in Hong Kong for GRs development and identify the different priority zones for deployment. The research acts as a decision-making tool for urban planners and managers to analyze the potential of green roofs and prioritize the use in social-economically hot-spot areas. The government shall be empowered by a knowledge package providing an overview of general approaches, GRs deployment zones, a quantitative understanding of the environmental/social

benefits, and practice priority development guidelines for public awareness, even though these are still not net benefits as the cost and institutional barriers are not considered

香港是一個高度密集的城市，由於快速的城市化和氣候變化帶來的風險日益增加，社會、經濟和環境部門承受著越來越大的壓力。人口發展導致的溫室氣體排放量已達到前所未有的高水平，是全球變暖的一個重要因素。減緩氣候變化，建設宜居、可持續的城市成為社會的主要共識。為了鼓勵香港使用低碳設施和技術，綠色屋頂等解決方案經常在智慧和可持續城市的背景下提出，因為它們提供了一種多功能和以解決方案為導向的方法來解決當前的問題挑戰。綠色屋頂與具有大量不透水表面的高度緊湊的城市密切相關。綠色屋頂不僅提供額外的綠地，還可以改善城市景觀並減弱城市熱島效應。具有大型屋頂的建築物通常由政府或商業機構所有，使得這些建築物更適合屋頂綠化改造。自 2001 年起，香港政府將屋頂綠化設計納入新的政府建築項目，同時在現有建築物的屋頂工程中引入改造屋頂綠化。

本項目旨在利用香港地理空間數據基礎設施的完善智慧城市平台，包括土地使用地圖、3D 建築模型/地籍、輔助三級規劃數據、衛星圖像和機載激光雷達數據，以確定可用的屋頂區域來容納綠色屋頂系統，並量化部署到香港的總體效益。我們使用屋頂的平面度、面積和坡度以及建築物的建築結構等參數來確定城市尺度上綠色屋頂的潛在位置。開發區域的優先順序是根據環境、交通、建築屬性、生態和社會經濟等因素確定的，因為綠色屋頂的實施具有高度優先性，但對於社會經濟貧困地區的居民來說可能負擔不起。項目完成後，它提出了香港超過 312,170 棟建築物屋頂的潛在利用率，以供綠色屋頂開發，並確定了不同的優先級部署區域。本研究可作為城市規劃者和管理者的決策工具，分析綠色屋頂的潛力並優先在社會經濟熱點地區使用。政府應獲得知識包的授權，該知識包概述一般方法、綠色屋頂部署區域、對環境/社會效益的定量理解以及提高公眾意識的優先發展指南, 儘管這些還不是淨收益，因為沒有考慮成本和體制障礙。

2) Layman Summary on Policy Implications and Recommendations

1. About 90% of the total roof area can be green retrofitted in Hong Kong by considering the building age and roof slope, planarity and size, and ~73% of roof areas show urgency for greening ($priority \geq 0.7$) based on environmental, meteorological, building planning attributes ecological, transportation and social-economic criterion.

2. Green roofs can raise the average greenspace coverage rate around buildings from 0.35 to 0.58 and increase human exposure to greenspace index value from 35.3% to 56.7%.
3. Green roofs can drop the air temperature by from 0 - 0.4℃ and save electricity energy by about 4.68×10^{8} kW · h in one year.
4. The annual equivalent of carbon emissions reduced by green roofs is about 1,010,000 metric tons, which is equivalent to offsetting about 3% of annual carbon emissions in Kong Hong.
5. Green roofs could bring in a total annual economic value of around HK$ 669.4 million through energy saving and carbon emission reduction.
6. Geospatial big data analytics shows the high effectiveness for the city-scale assessment of roof greening priority and benefits at an individual building level in Hong Kong.

1. 在考慮到建築年齡和屋頂坡度、平面度和尺寸，香港約 90%的屋頂總面積可進行綠化改造，綜合基於環境、氣象、建築規劃屬性、生態、交通和社會經濟標準, 約 73%的屋頂面積表現出綠化緊迫性（優先級≥0.7）。
2. 綠色屋頂可以將建築物周圍的平均綠地覆蓋率從 0.35 提高到 0.58，並將人類接觸綠地指數值從 35.3%提高到 56.7%。
3. 綠色屋頂一年可降低氣溫 0-0.4℃，節省電能約 4.68×10^8 kW·h。
4. 綠色屋頂每年減少的碳排放量約為 1,010,000 公噸，相當於抵消香港每年約 3%的碳排放量。
5. 綠色屋頂每年可通過節能減碳帶來約 6.694 億港元的總經濟價值。
6. 地理空間大數據分析顯示，其在香港城市規模個別建築物層面對屋頂綠化優先事項和效益進行評估上具有很高的有效性。

1. Introduction

Unprecedented urbanization along with the global climate change has led to sustained pressure on social, economic and environmental aspects of the cities, which has been significantly influencing the human life and the natural environment (Stephenne et al., 2016). Energy use pattern and environmental issues induced by the rapid growth of population and high-density of buildings in metropolitan and their consumption-driven lifestyles prove to be a big challenge for urban governors and planners (Dizdaroglu et al., 2012; Wu, et al., 2018; Aboelata 2021). In such a situation, urban governance is redirected towards the frontier of sustainable and low-carbon cities (Sodiq et al., 2019).

Nature-Based Solutions (NBS) are proposed in the context of sustainable urban development, which present a multi-functional approach by addressing social, economic and environmental sustainability issues simultaneously (Dorst et al., 2019). Urban Green Infrastructure (UGI) including green roofs (GRs) is one key element of the NBS which are high relevance to urban areas due to abundance of impervious surfaces i.e., building roofs (Shafique et al., 2018). Moreover, it is difficult for high density cities with compact nature of the built environment such as Hong Kong to implement other kinds of large-scale UGIs such as planting roadside trees and developing urban green spaces. As one type of UGI, green roofs positively contribute to sustainable and carbon-neutralized cities and remain a sustainable alternative to conventional roofs. They are defined as the living vegetation installed on the building rooftops (Guzmán-Sánchez et al., 2018), consisting mainly of two types of green roofs, intensive and extensive (Peng & Jim, 2015). Intensive roofs are characterized by a thick layer of substrate with a variety of plants whereas extensive roofs are lightweight and equipped with a thin layer of substrate. Most of the previous works have concentrated on implementation of extensive green roofs as per lower installation and maintenance costs incurred.

Furthermore, green roofs have a potential to provide multiple urban ecosystem services (Hoeben & Posch, 2021) and enhance the urban biodiversity such as mitigation of heat island, regulation of microclimate and provision of a better quality of life, etc. (Sharma et al., 2018; Langemeyer et al., 2020). Energy saving through incorporating green roof features and the use of energy efficiency technologies can be also realized to achieve sustainability. The benefits of GRs system include but are not limited to the fowling:

Environmental benefits:

- Mitigate urban heat island and improve air quality
- Create natural habitat and increase biodiversity
- Insulate and absorb sound

Economic benefits:

- Improve roof durability
- Reduce building cooling load and energy costs
- Provide open space and increase property value

Social benefits:

- Aesthetic for city space
- Provide community green space for sports & leisure
- Community participation

Moreover, since the development of the GRs system can help reduce the carbon stock in the atmosphere by carbon capture functions, it even contributes more to carbon neutrality in HK city by earning carbon credits. Carbon Credits are introduced by CLP company of HK and supposed to generated from renewable sources instead of fossil fuels and can be used to offset carbon emissions by other parties. A carbon credit represents one metric ton of carbon emissions that is avoided by completing an activity in a less carbon intensive way, such as carbon captured by the photosynthesis process of GRs.

With a potential social acceptance (Lee & Jim, 2018), green roofs can be incorporated at a city scale with the help of municipal departments. Thereby, green roofs associated with multi-dimensional benefits could assist in sustainable urban development toward carbon neutrality. However, due to different construction types of buildings and rooftops, not all the buildings are able to accommodate the green roof strategy. Meticulous urban development in a heterogeneous city environment requires different GR strategies. Hence, identification of the high-potential areas for mobilizing the green roofs across a high-density city is an essential prelude to its implementation. Apart from this, Hong Kong has witnessed an unequal distribution and development of green spaces. This not only unbalances the life quality of citizens but also results in a discontinuity in green spaces affecting the biodiversity. Moreover, there is a spatial variation of building density and functional distribution which also leads to varied temperature in different parts of the city (Sharma et al., 2016). Additionally, socio-economic inequalities in cities worldwide are a big problem since the rapid urbanization process (UN-Habitat, 2012). Socio-economically deprived regions are characterized by a low quality of life as a result of the existing social-economic segregation and environmental problems (Gou et al., 2018). As UGIs and green roofs are supposed to deliver multiple benefits, it is important to identify potential locations and prioritize their implementation in order to leverage multiple benefits according to different policy focuses.

Back to early time of 2007, architectural services department of HK government has published a preliminary report of "STUDY ON GREEN ROOF APPLICATION IN HONG KONG", which has focused on technical specifications and guidelines for designing and installing green roof systems in HK as well as cost analysis. In the past decade, many studies have been conducted to identify the potential of green roofs at various scales of cities across the world. Building characteristics comprising roof slope, area, orientation, and planarity are mainly used for identifying the development locations for green roofs (Karteris et al., 2016; Mallinis et al., 2014). Langemeyer et al. (2020) focused on identifying priority areas for implementing GRs based on optimizing the provision of ecosystem services, which include thermal regulation, runoff control, biodiversity, social cohesion and recreation. Herrera-Gomez et al. (2017) particularly identified the areas where green roofs can be retrofitted to mitigate urban heat island effect. As it is important to combine the identification of potential of green roofs with priority analysis, Silva et al. (2017) integrated the building characteristics with existing greenness and population density to ensure the expansion of urban greenness to the areas wherever mostly needed. A similar approach is used by Grunwald et al. (2017), in which ecosystem services: improvement of urban air quality, climate regulation, water retention and biodiversity enhancement are adopted to determine priority areas for GRs deployment.

The evaluation of roof greening priority commonly involves three steps: identification of potential roofs, selection and measurement of indicators, and calculation of greening priority (Xu et al., 2021). Building attributes such as age, roof slope, and roof area, are often used to identify the potential roofs that can be greened retrofit. Previous studies obtained building attributes from on-site measurements or government records (Silva et al., 2017), thus, focusing on the evaluation at a small scale (Hong et al., 2019). High-resolution aerial and satellite remote sensing data enable urban-scale greening evaluation. Accordingly, some building attributes collected from remote sensing and building census data are further used to establish appropriate roof greening indicators (Grunwald et al., 2017), and then the greening priorities of potential roofs are calculated by combining these indicators. However, as mentioned earlier, green roofs are associated with multiple factors, so that only building attributes are inadequate to scientifically prioritize green roofs (Hoeben & Posch, 2021; Shafique et al., 2018). Additionally, although roof greening can reduce the adverse effects of urbanization, most existing studies are limited to the discussion of a specific benefit (He et al., 2020; Shafique et al., 2020). Overall, there are few studies assessing the priority of building roof greening and the combined effects on environments, climate changes, and social economy from the perspective of urban sustainable development, especially since a comprehensive assessment on the urban scale is still blank. A full understanding of priorities and benefits is, therefore, necessary to facilitate green roofs at urban scale.

In this regard, we analyze the potential of green roofs in Hong Kong, a thoroughly urbanized city with a population density of 25,684 people per square kilometer (Demographia, 2022), and the median living space per capita among the smallest in the world (Wong et al., 2019). Despite the high proportion (about 0.7) of greenspace areas across Hong Kong, the greenspaces are uneven, in which human exposure to greenspace is only 0.35 (Chen et al., 2022). Moreover, Hong Kong is located in the subtropical region, where high-density buildings and large amounts of hard impervious surfaces lead to increased solar absorption and evapotranspiration reduction, resulting in the prominent UHI effect, meanwhile, intensive anthropogenic activities have increased urban carbon emissions. As a result, the contradiction between urbanization and human well-being is increasingly fierce in Hong Kong. To develop urban sustainability, thus, we undertook an urban-scale evaluation of roof greening. Here, we used geospatial big data to comprehensively evaluate the priority and benefits of roof greening from the perspective of urban sustainability and overcome the limitations of separate evaluation of small-scale green roofs based on limited data and indicators, thereby enhancing the cognition of green roofs. Specifically, geometry and attribute information were used to identify potential green roofs, rather than directly to assess greening priorities; different from the indicators based on building attributes, we focused on several indicators closely related to urban sustainability and quantified them to determine the urgency of roof greening under different conditions, then combined all indicators to evaluate the greening priority of each potential roof. Furthermore, a comprehensive benefit of green roofs in urban sustainability was assessed. This study suggests a reproducible way to prioritize green roofs at an urban scale, meanwhile, can provide reference to city planners and public decision-makers.

2. Objectives of the Study

1. Identifying potential candidates for installing green roofs in Hong Kong using geospatial intelligence technology

2. Prioritizing development zones for green roofs in Hong Kong based on multi-criteria decision analysis to accommodate diverse geospatial, socio-economic and environmental factors.

3. Quantifying and validating functional benefits of the prioritized green roof zones and assessing factor relevance using numerical simulation toward policymaking

4. Leveraging geospatial data infrastructure and smart city techniques in Hong Kong

3. Research Methodology

To support urban sustainability in Hong Kong, an entire research flowchart of prioritizing green roofs was designed in Fig. 1. We combined airborne laser scanning point clouds, Google maps, and building census data to obtain building attributes (such as roof slope, area, and building age) and extract building roofs, and then determined potential roofs that can be greened. Subsequently, we constructed six indicators (including greenspace rate, distance to main road, building category, median monthly income, surface temperature, and annual precipitation) for prioritizing green roofs from the three aspects of ecological environment, socio-economy, and meteorology, meanwhile, we supplemented satellite remote sensing images, road network data, weather station observation data, and government statistical data to quantify these indicators. We further assess the benefits of green roofs on environments, urban heat mitigation, carbon emission reduction, and social economy through simulation and estimation.

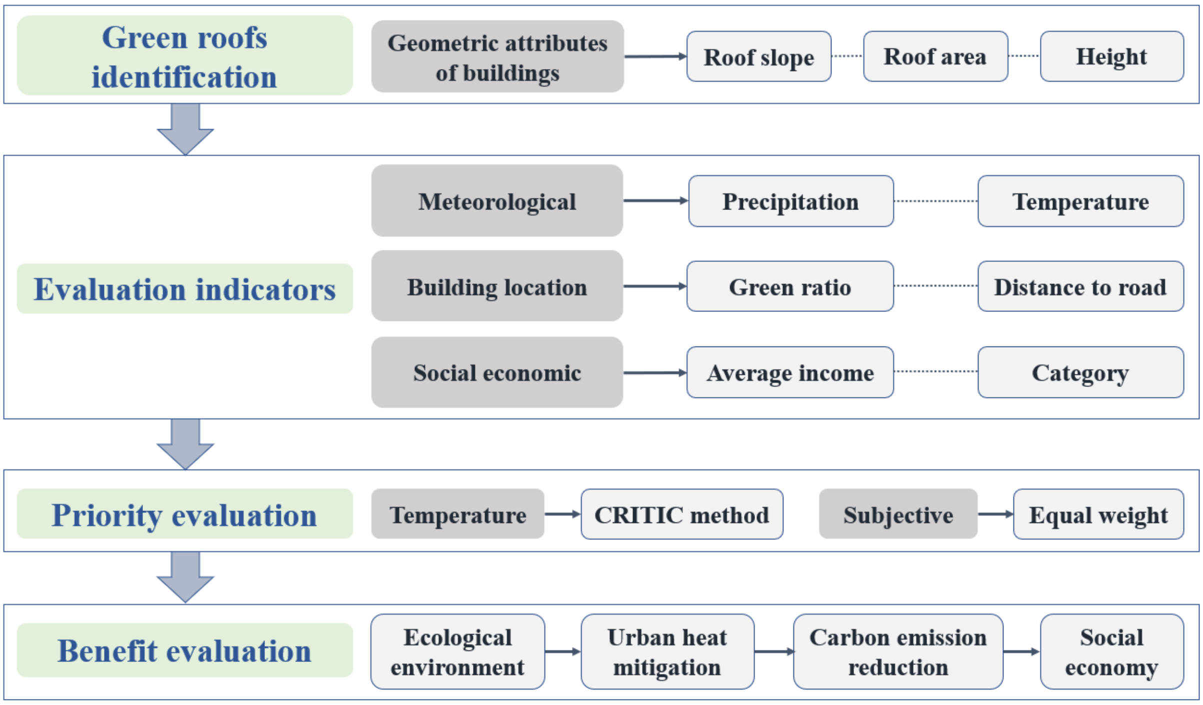

Fig. 1 The overall flowchart of this study, including identification of potential green roofs, selection and measurement of greening indicators, and greening priority calculation.

3.1 Identification of building roofs

To realize the coupling of multi-source data, we detected all roofs from airborne laser scanning point clouds. First, a deep learning framework was proposed to perform semantic segmentation of point clouds and classify each object, including buildings, vegetation, and ground. Next, we detected and segmented roofs from building points, and then computed roof area, roof slope, and building height, for identifying potential green roofs. Furthermore, the building attributes, including building age and category, were extracted from satellite images through an improved deep learning network for image processing.

3.1.1 Semantic segmentation of airborne laser scanning point cloud

In this study, weak labels are defined as sparse labels randomly distributed across the scene. Assuming that the input points $\mathcal{P} \in R^{N \times D}$ consist of N points with D dimensional features, $M (M \ll N)$ points are assigned labels, denoted as $\mathcal{P}_w \in R^{M \times D}$. The corresponding labels $\mathcal{Y} \in R^M$ with K classes and unlabeled points are denoted as $\mathcal{P}_u \in R^{(N-M) \times D}$. To compensate for the lack of information caused by sparse annotations, a weakly supervised strategy has been proposed to take advantage of both labeled and unlabeled data. The workflow of the proposed method is illustrated in Fig. 2. Regarding the weak supervision, the calculation of the loss function and backpropagation was implemented only on few labeled points, following the scheme of fully supervised learning. Entropy regularization (ER) is adopted to exploit the information of unlabeled data, which minimizes class overlap and generates predictions with high confidence. In addition, an ensemble prediction constraint (EPC) is developed to enhance the robustness of the trained model by comparing the prediction at the current training step with the ensemble value. Moreover, we develop an online soft pseudo-labeling (OSPL) strategy to further improve the performance of the model.

KPConv (Thomas et al., 2019) is used in this study as a backbone network because of its state-of-the-art results on several open datasets. Moreover, KPConv resorts to the idea of convolution kernels from image processing by extending deformable kernel points to adapt to the local features of point clouds. We chose a rigid point convolution kernel and used the same network architecture as KPConv for our semantic seg-mentation task.

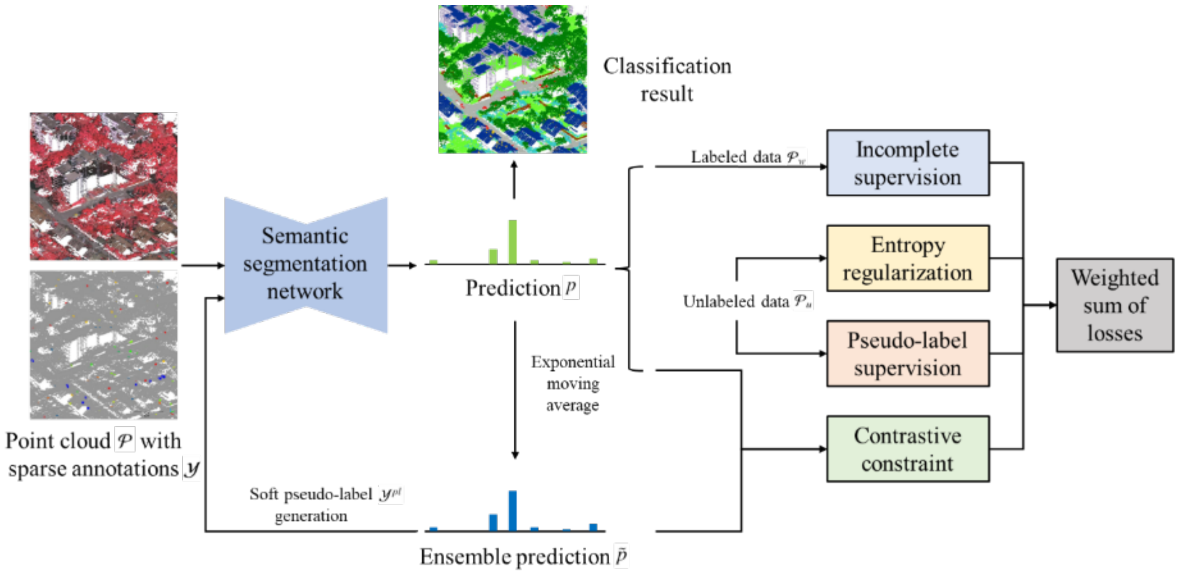

Fig. 2 Schematic diagram of the proposed weakly supervised strategy (Wang & Yao, 2022)**.**

3.1.1.1 Entropy regularization

To enlighten the idea of entropy regularization, we first introduce incomplete training on labeled data. The training process of incomplete supervision is similar to that of full supervision, and the only difference is the design of the loss function. Because only a small number of points $\mathcal{P}_w$ are provided label information, we calculate the loss of these points and perform backpropagation. The softmax cross-entropy is a commonly used loss function in supervised semantic segmentation of point clouds and is denoted as:

$$\mathcal{L}_{seg} = -\frac{1}{|\mathcal{P}_w|}\sum_{i}^{M}\sum_{c}^{K} y_{ic}\log p_{ic} \tag{1}$$

where p_{ic} is the predicted probability of point p_i and y_{ic} represents the cth category value of the one-hot vector of label $\mathcal{Y}_i$. Notwithstanding the lack of annotated information for loss calculation, we can take advan-tage of the class-wise posterior probability p_c of unlabeled points $\mathcal{P}_u$. This is referred to as the predictive probability inferred from the trained models. Entropy regularization (Grandvalet & Bengio, 2004) was proposed based on the conclusion that the information contained in unlabeled data decreases as classes overlap. Entropy H is a measure of class overlap and is invariant to the parameterization of the model, which is related to the usefulness of unlabeled data where prediction is ambiguous. Hence, this measure can be used to predict well-separated classes of unlabeled data. By reducing the class overlap, entropy regularization decreases the uncertainty and supplies predictions with high confidence. Given a target point cloud, the Shannon entropy (Shannon, 1948) of each point H_i is used, and is denoted as:

$$H_i = -\sum_{c}^{K} p_{ic} \log p_{ic} \tag{2}$$

Entropy regularization is proposed to minimize the entropy of the posterior probability, and the loss was calculated as an averaged value:

$$\mathcal{L}_{ent} = \frac{1}{|\mathcal{P}_u|} \sum_{i}^{N-M} H_i \tag{3}$$

The supervised classification loss $\mathcal{L}_{seg}$ and entropy regularization loss $\mathcal{L}_{ent}$ are calculated on labeled and unlabeled points, respectively, subject to simultaneous optimization during training.

3.1.1.2 Ensemble prediction constraint

In this section, a consistency constraint is proposed to enhance the model to produce more stable predictions. In the case of a lack of labels, the consistency constraint, as a self-learning method, refers to the minimization of the difference between a pair of well-planned contrastive samples. The motivation is based on the assumption that prediction p should remain unchanged when applying small perturbations s to target t, such as input data or model parameters, denoted as $p_t = p_{t+s}$. To generate effective contrastive samples, Temporal Ensembling (TE) (Laine & Aila, 2017) recorded the ensemble prediction $\tilde{p}$ during the training process and compared it with the prediction p at the current training step. Mean teachers (MT) (Tarvainen & Valpola, 2017) further derived ensemble model parameters to produce predictions for consistency constraints, in which the ensemble value was updated per step.

In this study, similar to TE, the ensemble value of predictions $\tilde{p}$ ss adopted, and the weakness of TE ss alleviated in the point cloud classification task using the overlapped mini-batch paradigm. In large-scale out-door point-cloud tasks, for which a mini-batch is created to represent small subsets of data. Considering the inevitable errors in the boundary region of the training samples, overlaps between subsets are required to enhance the feature representation ability. Furthermore, points within the overlapped areas of multiple mini-batch subsets are characterized by different global information, which can be regarded as point-wise data augmentation. Hence, one point can be fed into the network multiple times at each epoch. As shown in Fig. 3, the marked point is assigned to different mini- batches at different training steps (T_0, T_1, T_2, etc.). In this way, the ensemble prediction $\tilde{p}_i$ is updated multiple times per epoch, and the training efficiency is retained, as only one forward propagation is required at each step. For each point, the exponential moving average (EMA) was utilized to compute the ensemble prediction, which updated the variable related to its historical values. At each step, the ensemble prediction ˜p contained in the mini-batches was updated. The (t-1)th EMA value of point predictions as $\tilde{p}(t-1)$ will be updated subsequently as:

$$\tilde{p}(t) = \alpha \cdot \tilde{p}(t-1) + (1-\alpha) \cdot p \tag{4}$$

where α is the coefficient used to balance the weighting between the ensemble and new values, which is set to 0.9. The mean square error (MSE) is used to describe the consistency cost, denoted as:

$$\mathcal{L}_{epc} = -\frac{1}{|\mathcal{P}|}\sum_{i}^{N}|p_i - \tilde{p}_i|^2 \tag{5}$$

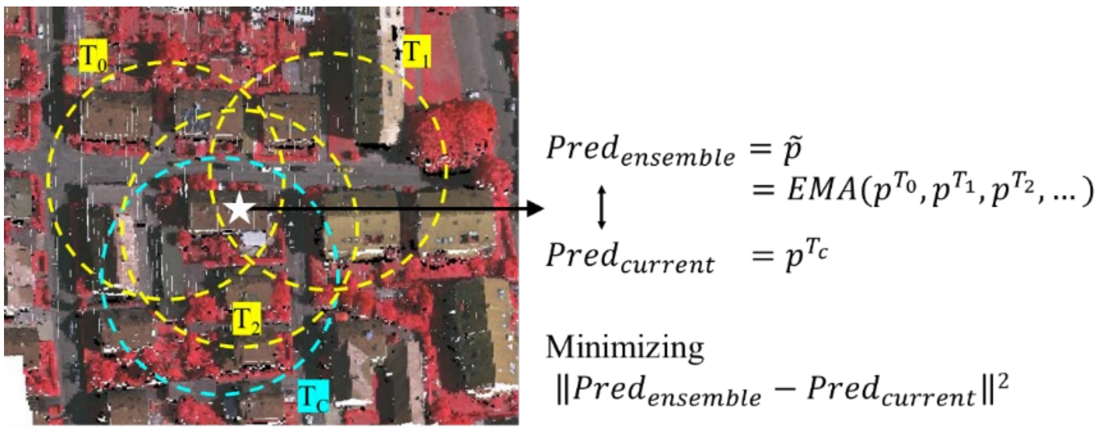

Fig. 3 Illustration of ensemble prediction constraint. The objective is to minimize the difference between the two predictions, as ensemble prediction is often referred to as a more robust estimation (Wang & Yao, 2022).

3.1.1.3 Online soft pseudo-labeling

As a simple yet efficient semi-supervised method, pseudo-label $\mathcal{Y}^{pl}$ can alleviate the problem of limited annotations. In the pseudo-label method, a classifier is trained to produce predictions and then retrained by taking inferred classes for unlabeled data as true labels. By increasing the number of pseudo-labels, we intend to reproduce class distributions in the feature space at the scene level. In this study, we propose an online soft pseudo-labeling method that enables all unlabeled points to be involved in pseudo-label generation without compromising training efficiency.

Generally, a prediction with high posterior probability is more likely to be correct. Thus, a commonly used method is to select labels with predicted probabilities exceeding a fixed threshold. However, it is difficult to select a generic threshold that is applicable to different datasets. To better reveal the class distribution and association across the entire scene, we derive and soften pseudo-labels on all unlabeled data $\mathcal{P}_u$ by associating them with different weights w based on class distribution uncertainty. In this study, the Shannon entropy of the predicted probability H is utilized to measure uncertainty, and a larger value represents higher uncertainty. We follow the strategy (Iscen, 2019), where the weight w_i for point pi is defined as:

$$w_i = 1 - \frac{H_i}{\log K} \tag{6}$$

Where $\log K$ is used to normalize w_i to [0, 1] according to the principle of maximum entropy.

We propose to use output predictions from each forward propagation directly to generate pseudo-labels. The ensemble prediction during training $\tilde{p}_i$ was utilized owing to its robustness and efficiency. Thus, hard pseudo-labels $\mathcal{Y}^{pl}$ from the unlabeled training data are generated as follows:

$$\mathcal{Y}_i^{pl} = \arg\max \tilde{p}_{ic}\, , i \in \mathcal{P}_u \tag{7}$$

We argue that true weak labels from the ground truth are essential for training the model. To retain their influence, the loss functions of the ground truth and pseudo-labels were formulated separately. The loss of pseudo-labels is calculated by weighted cross-entropy using instant predictions, denoted as:

$$\mathcal{L}_{seg}^{pl} = -\frac{1}{|\mathcal{P}_u|} \sum_{i}^{N-M} w_i \sum_{c}^{K} y_{ic}^{pl} \log p_{ic} \tag{8}$$

An illustration of the training processes of the two strategies is shown in Fig. 4. We contemporaneously generate and determine all pseudo-labels in a mini-batch from $\tilde{p}_i$ at each step, so its training process is performed quasi-equivalently to that of normal supervision, with retention of similar training time.

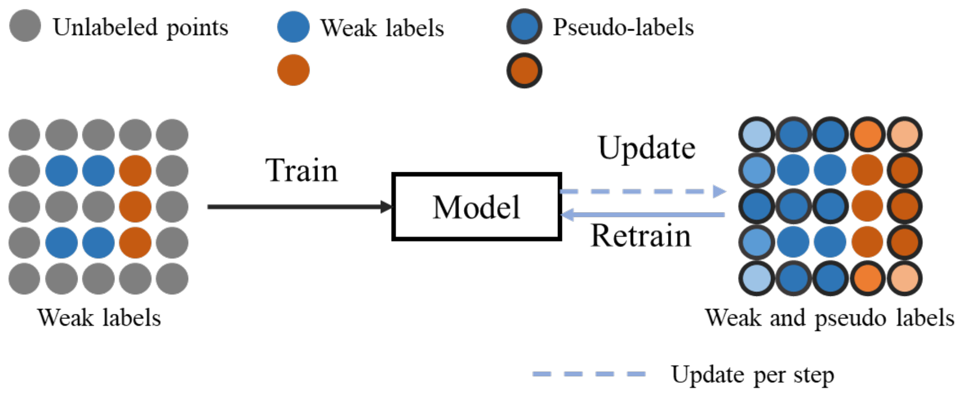

Fig. 4 An illustration of training process in online soft pseudo-labeling. OSPL updates the pseudo-labels of the training batch data per step. In addition, in contrast to crisp selection using a fixed threshold, OSPL assigns uncertainty-based weights to each pseudo-label, which are denoted by different color degrees (Wang & Yao, 2022).

3.1.1.4 Training process

All the losses proposed in the previous sections simultaneously participate in backpropagation with different weights. The combined optimization problem is presented as follows:

$$\Theta = \arg\min_{\Theta}\left(\mathcal{L}_{seg} + \lambda_{ent}\mathcal{L}_{ent} + \lambda_{epc}\mathcal{L}_{epc} + \lambda_{pl}\mathcal{L}_{seg}^{pl}\right) \tag{9}$$

where Θ represents the model parameters and λ_{ent}, λ_{epc}, and λ_{pl} are weighting factors. A ramp-up weight for unsupervised loss components was used in this study. Specifically, λ_{ent} and λ_{epc} are set equal in our experiments, defined by a Gaussian curve $\exp[-5(1-T)^2]$ following (Tarvainen & Valpola, 2017), where T increases linearly from 0 to 1 during the ramp-up period and λ_{pl} is set to zero during the ramp-up period. Therefore, the entire training process consisted of two stages, with each stage lasting for 100 epochs. Stage 1 is the ramp-up period, and λ_{ent}, λ_{epc}, and λ_{pl} are all set to 1 during stage 2.

3.1.2 Identification of potential green roofs

In this study, we defined the uppermost covered part of a building as the roof. Thus, we projected all building points into the horizontal plane and regarded the highest point at each position as a candidate roof point. Then, we filtered out edge and wall points by the elevation difference between each candidate roof point and its 4-neighboring points, and the point is considered a roof point if the difference is small (Fig. 5a). After detecting roof points, we segmented roof points based on region growing algorithm (Shao et al., 2021) and computed the slope and area of each segment, the segment with slope less than 15 degrees (Fig. 5b) and area more than 10 m^2 (Fig. 5c) were regarded as potential roofs that can be greened.

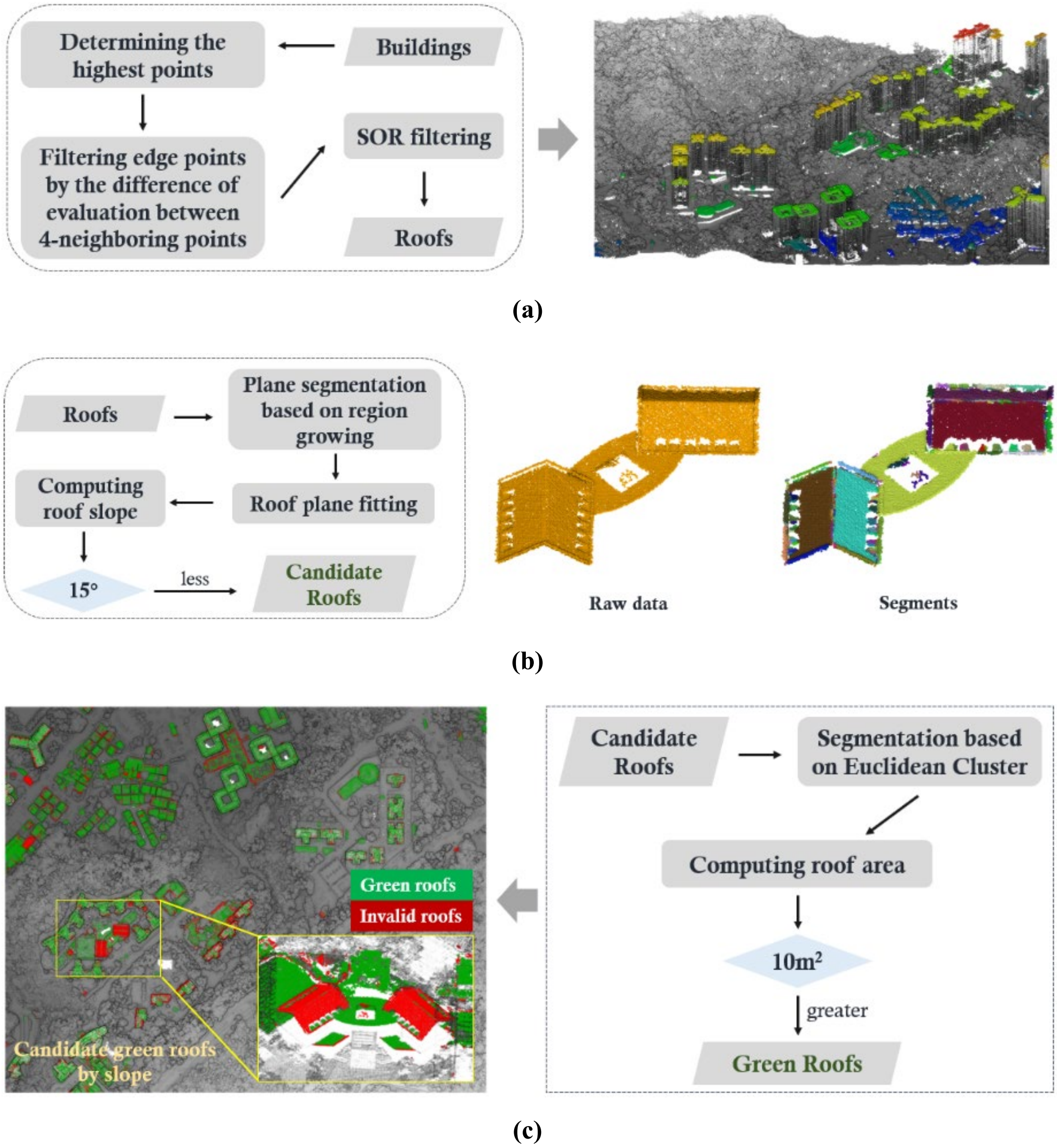

Fig. 5 Identifying potential green roofs from building point clouds. **a**, extracting roofs from building point cloud; (**b**) and (**c**) Detecting potential green roofs through roof slope and roof area.

3.1.3 Extraction of building attributes

Building age and category were two important factors of prioritizing green roofs, but many buildings lacked information on the two factors. Therefore, we predicted the age and category of these buildings using a deep learning network to image super-resolution. We first fused the geographic data that record information on more than 400,000 buildings and Google Maps data through the geographic reference information, and cropped the image corresponding to each building from Google Maps according to the building footprint; second, we input images of buildings with the age and category information into a deep learning network as training samples (about 31,500 buildings with age and 150,000 with category), and referred the images of buildings without age and category as test samples. We classify the buildings in Hong Kong into 11 main categories according to their functions (commercia and office, education institution, high private, industrial, low private, medical, mixed-used, public house, public services, recreation, religion), with each category containing 10,000 images and there are 11,000 images in total, and there are divided into five categories according to the time of construction (before1970, 1970s, 1980s, 1990s and after 2000).

Building fine-grained categories and ages classification using low-resolution overhead images, this task faces huge challenges due to the low resolution and overhead view limitation of high-altitude satellite images and urban buildings across multiple fine-grained categories and ages exhibit significant variations in the number and distribution, leading to class imbalance problem. To address these issues, we propose a new approach to fine-grained classification of urban buildings from low-resolution overhead imagery in two steps. As shown in Fig. 6, in the first phase, we introduce a Denoising Diffusion Probabilistic Model (DDPM) (Ho et al., 2020; Sohl-Dickstein et al., 2015) based super-resolution method to enhance the quality of low-resolution satellite images. This approach leverages the transfer of features across different domains to improve the visual quality and level of detail in the images, enabling more accurate building classification in the next phase. In the second phase, we develop a new fine-grained building classification network with two improvements: Category Information Balancing Module (CIBM) and Contrast Supervision (CS) technique. The CIBM module addresses the issue of class imbalance by adaptively adjusting the weights of different building categories, ensuring a more balanced class representation in the training process. Additionally, the CS technique provides contrastive learning-based supervision sources, enabling the network to capture more discriminative features for improving classification accuracy.

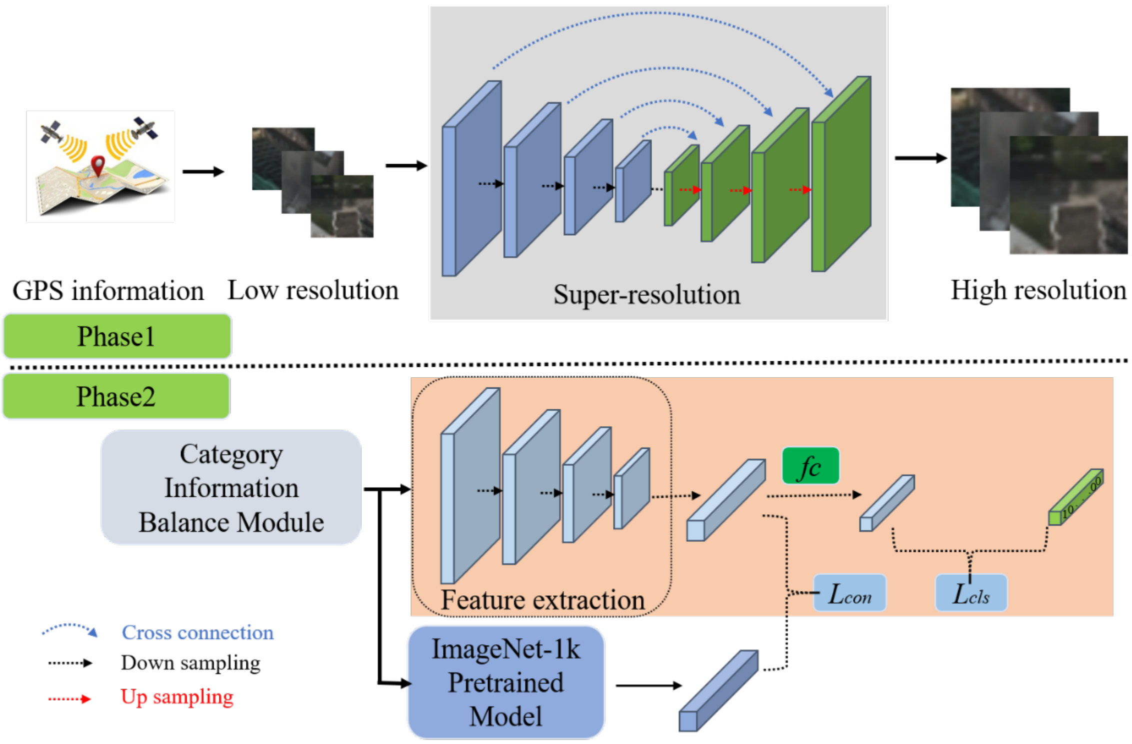

Fig. 6 Overview of our proposed building category fine-grained classification network based on low resolution overview images.

The leftmost column (Fig. 7) is an example of building low-resolution images we cropped from raw Google Maps data, with size of 32×32. And the next three columns are images after 3-fold super-resolution processing by Bilinear interpolation, Generative Adversarial Network (GAN) (Goodfellow et al., 2014; Karras et al., 2018), and DDPM methods respectively, there size are 128×128. By comparing these higher-resolution images, we can see the architectural features are retained or enhanced more prominently by the DDPM method, which lays the foundation of the feature information for the subsequent fine classification of the image.

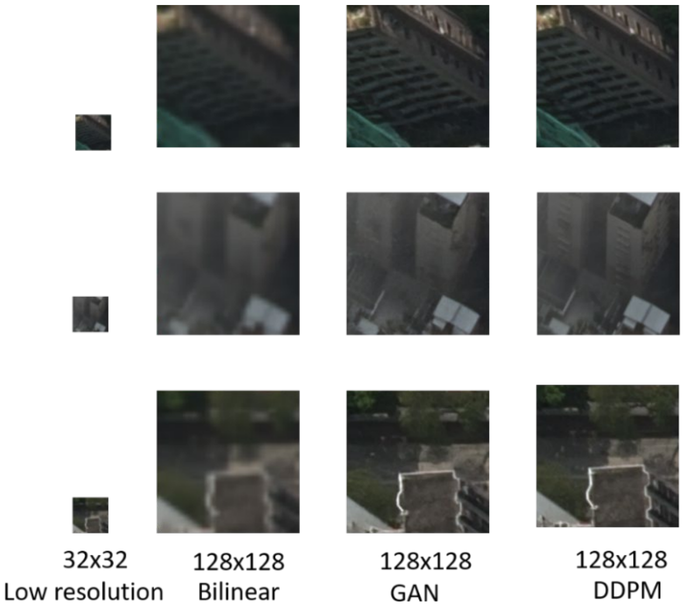

Fig. 7 Comparison of different super-resolution methods results for low-resolution overhead images.

Category unbalance is one of the most important and common problem in image classification task. There are many reasons for this problem, such as the fact that a certain category of data is more difficult to obtain than others, and the corresponding cost is much higher. In order to obtain the same results for a category with fewer samples as for a larger number of data categories, many scholars have proposed many different solutions to solve the widespread problem of category imbalance. Under-sampling is a common method which count the number of samples per category and calculate the weights for each category accordingly, with fewer samples receiving greater weights and vice versa, and adjust the number of samples per category input to the network by the weights during training, by reducing the number of categories with more data input to ensure that the samples input to each category are equivalent. Generative task networks, such as the Generative Adversarial Network (GAN), are another effective solution for this problem, where the number of samples input to the classification network is equal for each category by supplementing the category with a smaller number of samples. Although all of these approaches have achieved varying degrees of improvement, they only consider the problem of category imbalance in terms of the number of samples in all categories, but not in terms of the 'distance' or relevance between samples in each category. In our project, we proposed a new module which take the relevance between samples in each category, in the training phase we calculate new weights to each category, making the training process more focused on the differences between categories rather than purely on the number of images, helping to improve the robustness of the model.

As shown in Fig. 8, the green part (c) is a common way to consider the unbalance problem in terms of the number of samples, our proposed CIBM takes into account the cosine similarity information between samples of each category by adding features extraction and similarity calculation. We compared the relational differences between the traditional method of balancing categories by means of sampling and our proposed CIBM.

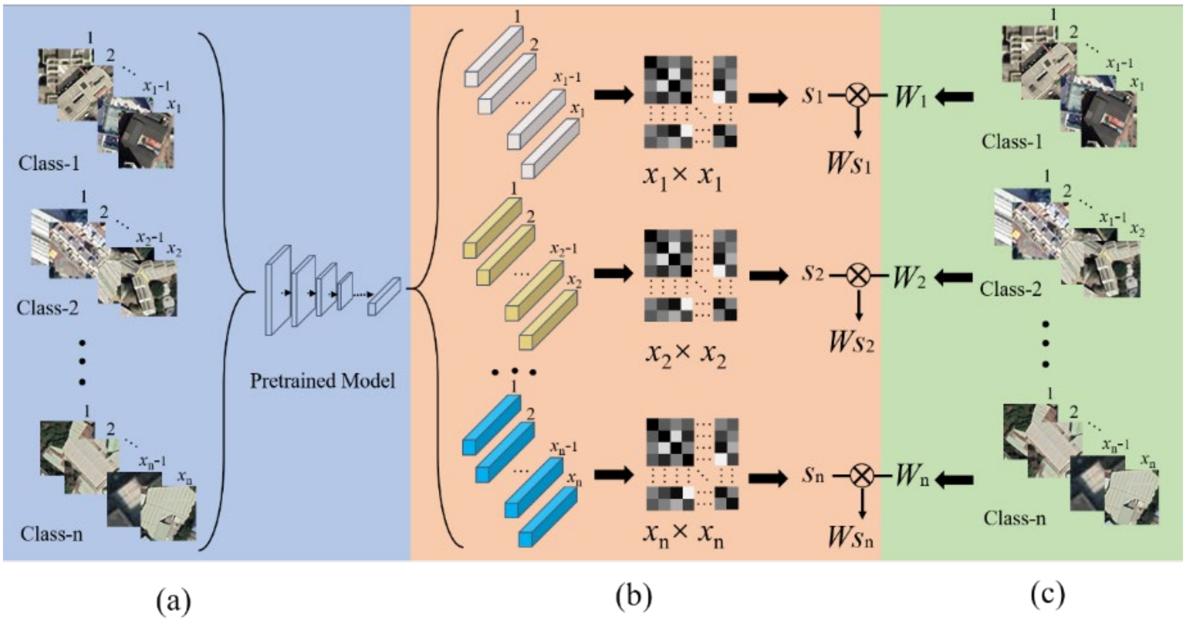

Fig. 8 Comparison of existing methods category information balanced module (CIBM). While the green part (**c**) in the figure is a common way to consider the unbalance problem in terms of the number of samples, our proposed CIBM takes into account the cosine similarity information between samples of each category by adding the blue area (**a**) and the orange area (**b**).

3.2 Measurement of indicator and priority

Quantifying the greenspace coverage around buildings is of great significance for the need to green roofs. Here, semantic airborne laser scanning point clouds were used to analyze the greenspace coverage. We projected all potential roof points and vegetation points into the horizontal plane at 5 m resolution and generated a map with a pixel size of 5 m × 5 m. Then, we calculated the greenspace coverage rate within a 500 m radius of each roof point according to Eq. (10) and set the average rate of all points on a roof as the final greenspace coverage rate of the potential roof.

$$GC = \frac{\sum_{i=1}^{n} G_i}{A} \tag{10}$$

where G_i represents the area (5 × 5 m^2) of a pixel, n is the total number of pixels that were covered by vegetation (such as trees and grasslands), A represents the area of a circle with a radius of 500 m, and GC is the greenspace coverage rate of a potential roof point.

To quantify the economic indicator, we combined the income data of 540 housing estates and all districts and applied the inverse distance weighted algorithm to obtain the distribution of median monthly income in 2021. For meteorological indicators, we first used the Google Earth Engine online platform to retrieve the surface temperature data at 30 m resolution for each season from Landsat 8 thermal infrared data (100 m resolution) and Landsat 8 multispectral data (30 m resolution), in which we selected a clear-sky image from each season to retrieve the surface temperature. However, there were clouds in summer and autumn satellite images. To remove the influence of clouds on the temperature inversion, we manually cut out the cloud in the images, and then supplemented the temperature of the cloud-occluded part through Kriging interpolation algorithm. Second, given the low resolution of the existing precipitation remote sensing data, we interpolated the annual precipitation data recorded by 139 meteorological stations in 2021 using the Kriging interpolation algorithm and obtained the precipitation distribution at 30 m resolution.

We assumed that each indicator has equal importance in urban sustainability, then the greening priority was calculated by an equally weighted index. Additionally, due to the difference in seasonal temperatures, we combined the temperature of the four seasons to measure the temperature indicator. Given the strong demand for cooling in the summer and autumn seasons with high temperatures, we gave the two seasons a higher prioritizing weight (0.4) than that in spring and winter (0.1):

$$\begin{aligned} P &= \frac{1}{6}\left(I_g + I_d + I_c + I_i + I_t + I_p\right);\ \left\{0 \le P, I_g, I_d, I_c, I_i, I_t, I_p \le 1\right\} \\ I_t &= \frac{1}{10}(T_1 + 4T_2 + 4T_3 + T_4);\ \{0 \le T_1, T_2, T_3, T_4 \le 1\} \end{aligned} \tag{11}$$

where P is the final priority of roof greening, $\{I_g, I_d, I_i, I_t, I_p\}$ are standardized prioritizing indicators and represent greenspace coverage rate I_g, distance between building and the nearest main road I_d, median monthly income I_i, the surface temperature I_t, and the annual precipitation I_p. I_c represents building category indicator. T_1, T_2, T_3, and T_4 are standardized temperatures of spring, summer, autumn, and winter, respectively. In the standardization process of prioritizing indicators, we defined I_t and I_p as positive indicators, and I_g, I_d, and I_i as negative indicators.

3.3 Benefit evaluation of green roofs

The common indicator of greenspace coverage does not consider accessibility by population (Song et al., 2021) and is difficult to quantify the connection between humans and natural environments. To overcome the shortcomings, human exposure to greenspace index value was used to reflect the exposure of residents to nature in the form of greenspaces, which is described by combining the population-weighted model and Eq. (10). We used the WorldPop data to quantify the population distribution in Hong Kong.

Weather Research and Forecasting (WRF) is a state-of-the-art mesoscale numerical weather prediction system, which can finely simulate the meteorological process of different types of cooling roofs on the urban thermal environment by coupling UCM. For the parameter setting of the WRF-UCM model, the albedo of bare roof was set to 0.15, and the greening area and the leaf area index were both set to 0; after roof greening, the albedo of green roof was set to 0.2, the area ratio of green roofs was set to 90%, and the leaf area index was set to 5. Moreover, the model used a double nesting setup with outer grid size of 300 m and an inner grid size of 100 m, and other parameters were in default. For each season, we simulated the air temperature distribution under three weather conditions, including sunny, cloudy, and rainy days.

We estimated the carbon stock based on the carbon density of the green roof per unit area (Eq. (12)), in which the carbon stock was from vegetation biomass and soil:

$$C = (d_v + d_s) \times A_r \tag{12}$$

where C represents the total carbon stock (g C), d_v and d_s represent the carbon density (g C·m^{-2}) of vegetation biomass and soil, respectively, and A_r is the area of the potential roofs (m^2). Given the greater carbon stock benefits of grassland ecosystems, we assumed that all potential roofs were covered by grassland and the soil depth was between 50 cm and 100 cm. Here, we experientially set d_v to 620 g C m^{-2} and d_s to 12 kg C m^{-2} according to literature reviews.

Vegetation absorption and energy saving are the two important functions that green roofs reduce carbon emissions. The capacity of the former is determined by the leaf area index and carbon sequestration per unit area of vegetation and can be expressed by:

$$C_v = W_{co2} \times LAI \times A_r \times 365 \tag{13}$$

where C_v represents the annual equivalent amount of carbon dioxide emission reduced by vegetation absorption (g ·a^{-1}), W_{co2} is the daily carbon sequestration per unit leaf area (g (m² ·d)$^{-1}$), and LAI is leaf area index. On the other hand, green roofs can save energy through thermal insulation, so the capacity of energy saving can be quantified by the reduced temperature using Eq. (14):

$$C_e = E \times k = \Delta T \times c_{air} \times m \times t \times k \\ = \Delta T \times c_{air} \times (d_{air} \times A \times h) \times t \times k \tag{14}$$

where C_e represents the annual equivalent amount of carbon dioxide emission covered by energy saving (g a^{-1}), E is the amount of annual energy saving through green roofs (kW ·h), and k is the conversion coefficient between electricity and carbon emissions, which represents carbon emissions produced by 1 kW h of electricity and is set to 0.79 kg (kW h)$^{-1}$. ΔT is the average temperature reduction (℃), c_{air} is air specific heat capacity (1004 J (kg ℃)$^{-1}$), m is the weight of the air contained in all buildings (kg) and is calculated by multiplying the air density d_{air} (1.29 kg·m^{-3}) and building volume (m^3), where the volume was estimated based on the product of the area (A) and average height (h) of all buildings in Hong Kong. The height of a building was calculated from the difference between the highest roof point of each building and the ground point with the nearest horizontal distance. t is the time (h) that electrical power needs to be used for cooling in one year. Accordingly, the total carbon emission reduction was estimated by adding C_v and C_e.

According to the carbon trading and electricity prices in Hong Kong, we further estimated the economic benefits of carbon emission reduction and energy saving. At the same time, we also analyzed the correlation between greenspace coverage rate and monthly income through linear regression and discussed the equity of different resident groups' access to greenspaces, thereby exploring whether green roofs have a positive effect on income.

4. Research Results/Findings

4.1 Data description

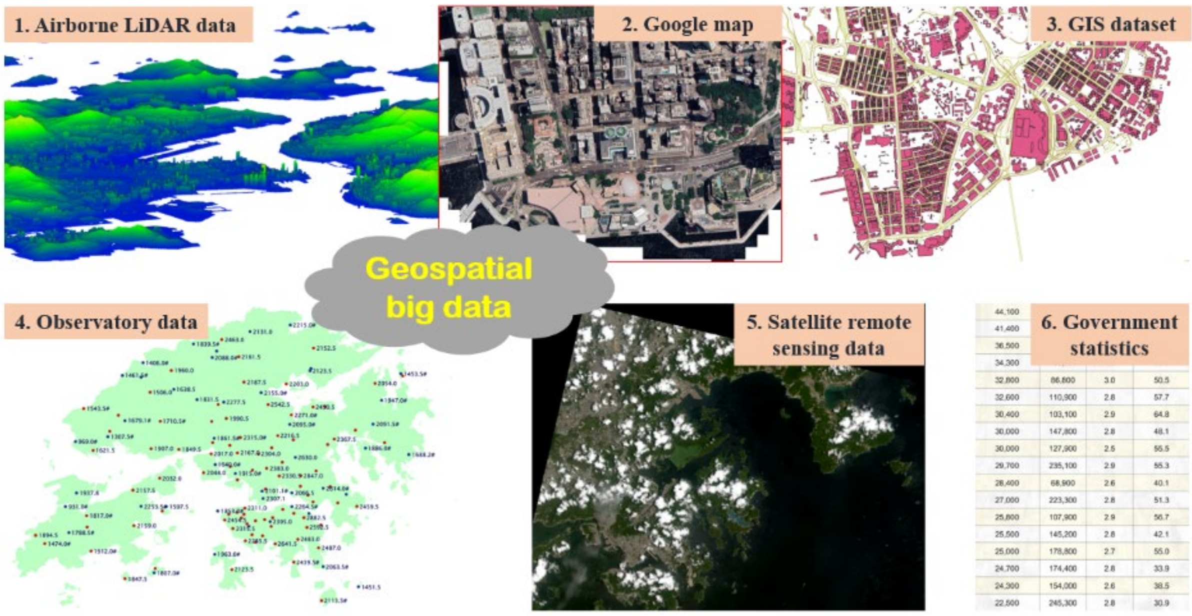

Fig. 9 Geospatial big data, including airborne laser scanning point cloud, Google Map data, geographic data of buildings and road networks, weather station observation data (precipitation), satellite remote sensing images, and government statistics.

Geospatial big data (Fig. 9), including airborne laser scanning point clouds, geographic data of building footprints and roads, Google Maps data, satellite remote sensing images, precipitation records, social statistics data, and population data, and were used to verify the feasibility. Specifically, we used airborne laser scanning point clouds (0.1 m resolution) to extract roofs and calculate roof slope, area, and greenspace coverage rate, used geographic data of buildings and main road networks to provide building attributes and analyze the distance between each building and its nearest main road, and used Google Maps image (0.8 m resolution) to predict the age and category of buildings. The satellite data acquired by Landsat 8 contained a total of 4 multispectral images (30 m resolution) from March 2021 to February 2022, which were used to retrieve the surface temperature of the four seasons. Precipitation in 2021 recorded by 139 weather stations were used to generate the precipitation distribution of the whole territory. The 2021 median monthly income data for each district and 540 housing estates counted by government were used to define the economic indicator. We further used to the population data from the WorldPop dataset (100 m resolution) for 2020 to compute human exposure to greenspace index value.

Geographic big data used in this study are available for download from the following sources: Airborne laser scanning point clouds and geographic data of building footprints and roads are from the Hong Kong GeoData Store (https://geodata.gov.hk/gs/); Google Maps data were obtained from the tile URL of Google Maps using QGIS software (http://mt0.google.com/vt/lyrs=s&hl=en&x={x}&y={y}&z={z}); Satellite remote sensing images are from the Landsat-8 data (https://landsat.gsfc.nasa.gov/satellites/landsat-8/); Building age information (https://initiumdata.carto.com/me) is from Hong Kong private building dataset; Annual precipitation records are from the weather stations (https://i-lens.hk/hkweather/); Population distribution of Hong Kong is obtained from WorldPop dataset (https://www.worldpop.org/); Median monthly income data are from 2021 Population Census (https://www.census2021.gov.hk/).

4.2 Potential green roofs

Given the rich spatial information, point clouds with a resolution of 0.1 m were acquired by airborne laser scanning in 2020 covering the entire Hong Kong and used to provide building roof attributes in this study. Building point clouds (Fig. 10a) were segmented based on a deep learning network, and roof points were then extracted from buildings (Fig. 10b). Next, roof attributes, including area and slope, were obtained from point clouds, where the roof with an area of less than 10 m^2 or a slope greater than 15 degrees is considered unsuitable for greening retrofit, meanwhile, a building older than 50 years will be considered insufficient in load-bearing capacity and its roof cannot be greened. Accordingly, potential green roofs were identified, and the roof area that can be greened reached 63.9 km^2, accounting for about 90% of the total roof area (70.1 km^2) in Hong Kong (Fig. 10c).

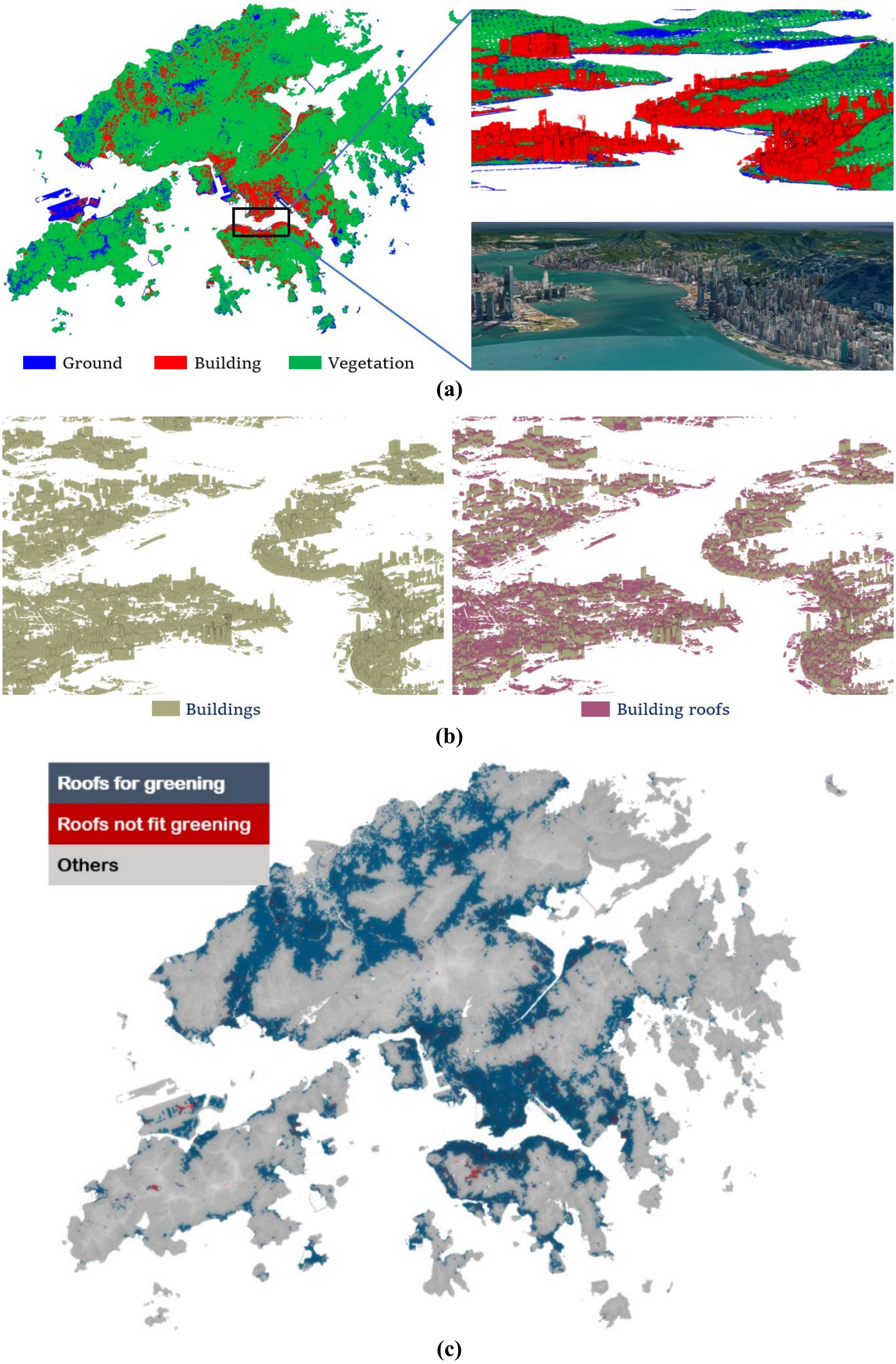

Fig. 10 Identification of potential green roofs. **a**, Semantic segmentation result of airborne laser scanning point cloud. **b**, Extracted building roofs. **c**, Potential green roofs in Hong Kong.

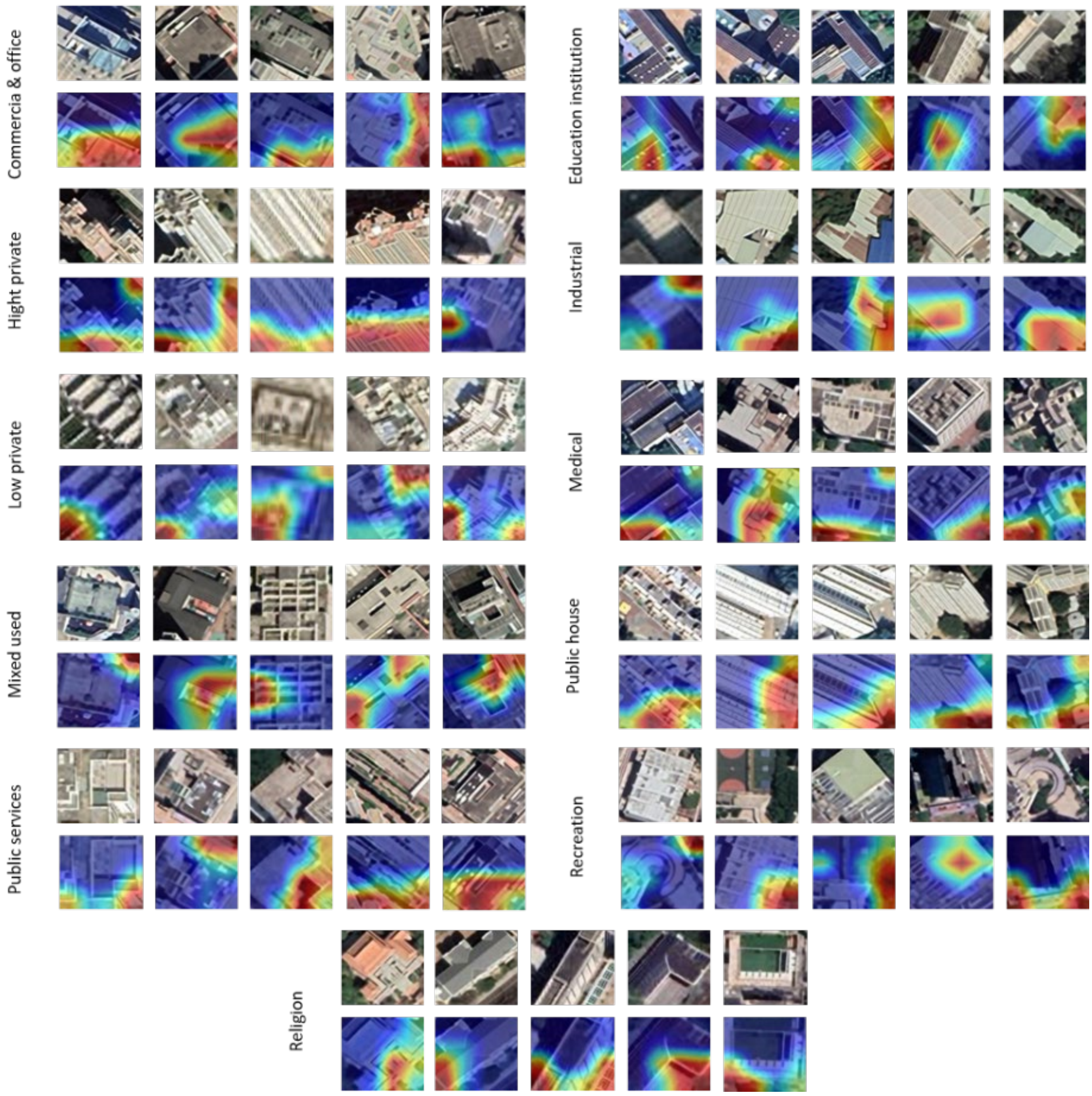

Fig. 11 Class Activation Mapping (CAM) of different building categories.

Fig. 11 shows the Class Activation Mapping (CAM) (Wonho et al., 2018; Tagaris et al., 2020) of different categories of buildings for our proposed method, through which we can know which part provide key feature information to our classification network in our fine-grained task. For example, the distinguished features of low private and medical buildings appear at the junction with the top and side. This is in line with our perception and reality, hospitals and low private buildings tend to have height restrictions and the sides will be styled differently from the rest of the building categories. And for industrial and recreational buildings, our network mainly focuses on the upper part of buildings or area, because the roof of industrial warehouses tastes different from that of other buildings, and a significant portion of the recreational facility area may have specific equipment or open area, it suggests that the categorical feature information extracted by our network is effective.

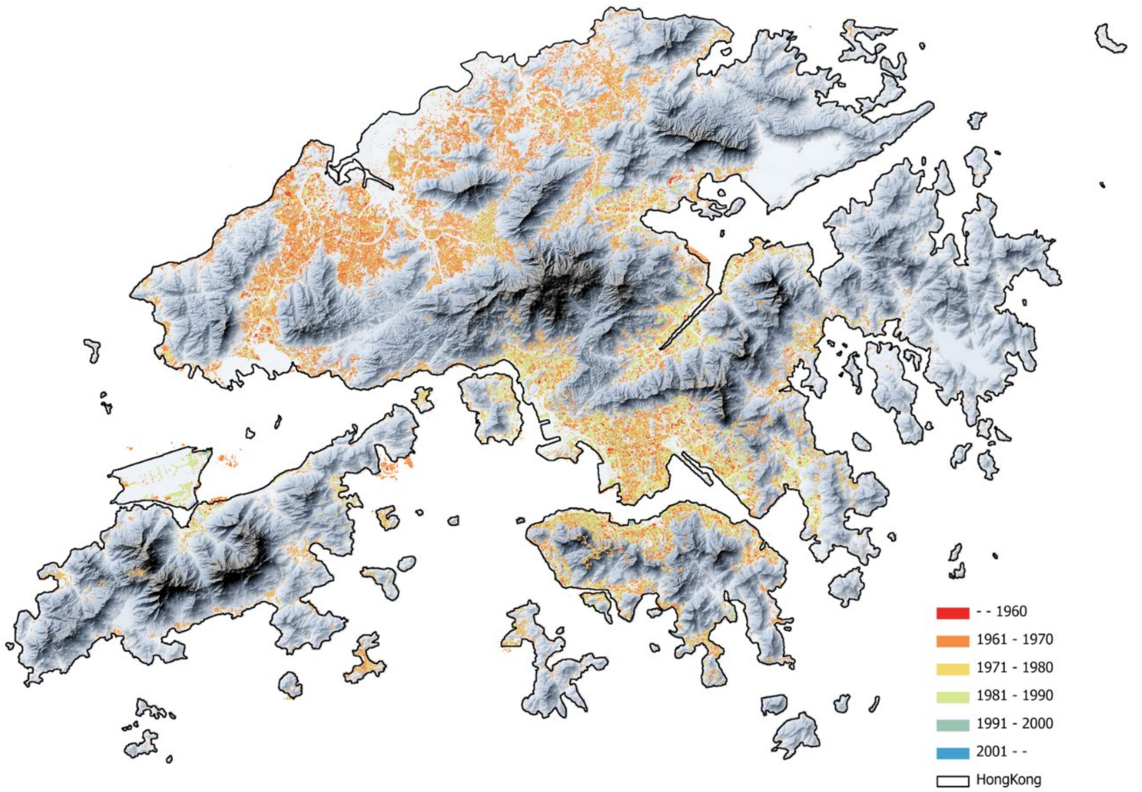

Fig. 12 The distribution of building age in Hong Kong.

From Fig. 12, most buildings are over 30 years old, and most of them are built in the 1970s and 1990s. Thus, the aging problem of buildings is serious in Hong Kong, which poses challenges to the promotion of green roofs in the future.

4.3 Indicators of greening priority

We focused on factors related to urban sustainability and designed six indicators to evaluate roof greening priority from three aspects: environmental, socio-economic, and meteorological factors.

In the environmental aspect, the relationship between buildings and the surrounding environment has important guiding significance for roof greening. In general, buildings far away from greenspaces have more need for green roofs than those surrounded by greenspaces (such as parks), here the greenspace coverage rate was used to quantify this assumption. We leveraged the semantic point clouds to quantify greenspace coverage rate within a 500-meter radius of each roof (Fig. 13a). Built-up areas with high-density buildings have a low greenspace coverage rate, especially in Kowloon and Hong Kong Island, where the rate is almost below 0.2, while the rate will increase to 0.5 or even more as it approaches the edge area adjacent to the vegetation. Apparently, buildings in the built-up area should be given a higher priority for roof greening. Additionally, considering the benefits of green roofs in absorbing vehicle exhaust and noise, the closer the building is to the main road, the more the need for roof greening. From the horizontal distance distribution of the building to the nearest main road (Fig. 13b), buildings in the build-up areas are generally closer to main roads and should be given higher greening priority.

In the socio-economic aspect, two indicators, building category and median income, were selected to assess the priority. The category indicates the social ownership of the building, including private (such as business buildings), public (such as government offices), and miscellaneous buildings. Due to the high capital costs, private house owners may be less enthusiastic about green roofs, so we set the greening priority of private buildings to 0.5. On the contrary, public buildings can actively respond to sustainable development policies, so the greening priority was set to 1. Miscellaneous category fall between private and public categories with a priority of 0.75. From Fig. 13c, miscellaneous and private buildings account for the majority in Hong Kong, where private buildings are concentrated in Kowloon and Hong Kong Island, and miscellaneous structures are in the New Territories. On the other hand, some studies implied a correlation between greenspaces and urban economies (such as per capita income), so median income was used as an indicator. Based on the median monthly income of 540 housing estates and each district released by the Hong Kong government in 2021, the distribution (Fig. 13d) of the median income was produced. Here, we assumed that greenspaces have a positive effect on raising resident income, so buildings in the low-income area will be given higher priority.

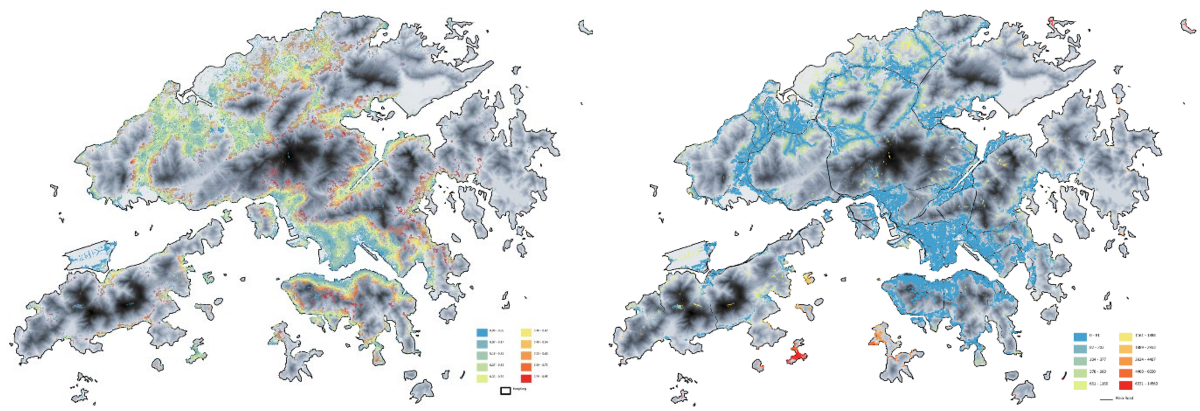

(a) (b)

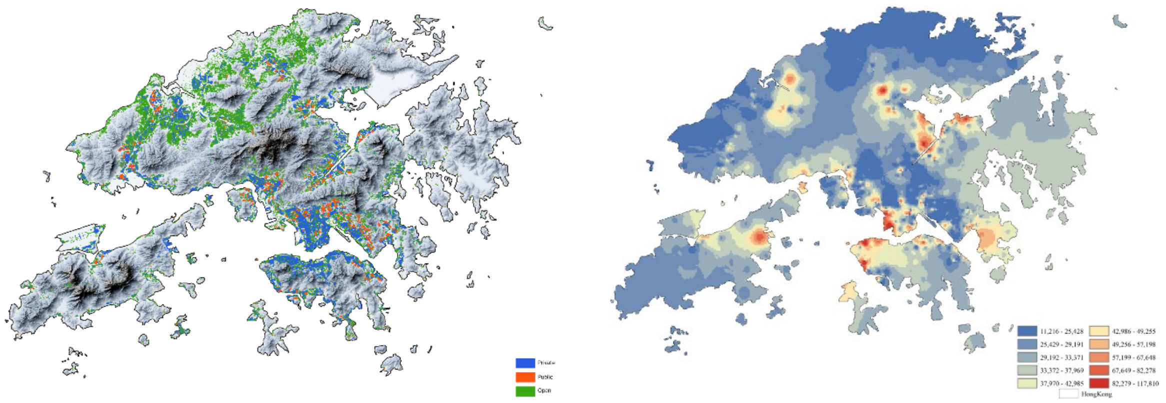

(c) (d)

Fig. 13 Priority indicators of roof greening in Hong Kong. **a**, Greenspace coverage rate within a 500 m range of buildings. **b**, Distance of each building to its nearest main road. **c**, Distribution of different categories of buildings. **d**, Median monthly income distribution by interpolating the income of 540 housing estates and each district in year 2021.

Hong Kong has an oceanic subtropical monsoon climate, especially hot and rainy in summer. Given the benefits of green roofs on surface temperature reduction and stormwater retention, we took temperature and precipitation as two appropriate indicators for prioritizing green roofs, and then used remote sensing data and weather station observation data to produce the distribution of temperature and precipitation in 2021. Specifically, owing to the temperature difference between different seasons, we used multi-temporal Landsat-8 images to invert the average temperature for each season, and at the same time, combined with the climate characteristic of Hong Kong, we designate March to May as spring, June to August as summer, September to November as autumn, and December to February as winter. In Fig. 14a, the temperature in build-up areas was generally higher than that in the vegetated suburbs and remote areas, so the UHI effect was significant, resulting in a higher priority for roof greening. Moreover, summer and autumn commonly show higher temperature, so should be given higher weight. Similarly, areas with high precipitation, such as Kowloon and Hong Kong Island (Fig. 14b), have more urgent needs for stormwater retention, so higher greening priority will be given to building roofs in these areas.

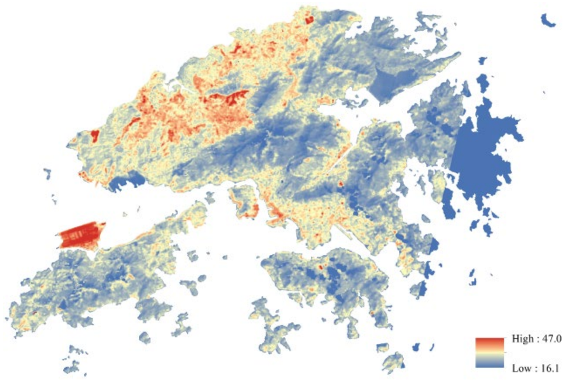

(a1) spring

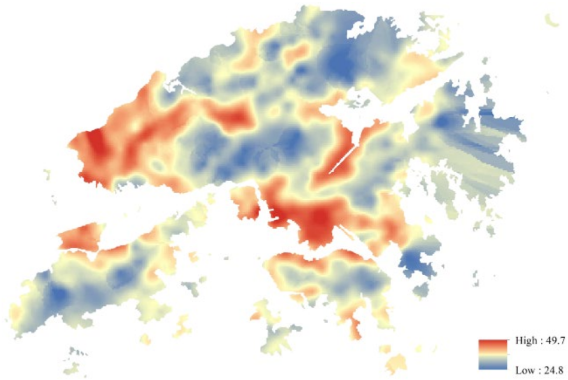

(a2) summer

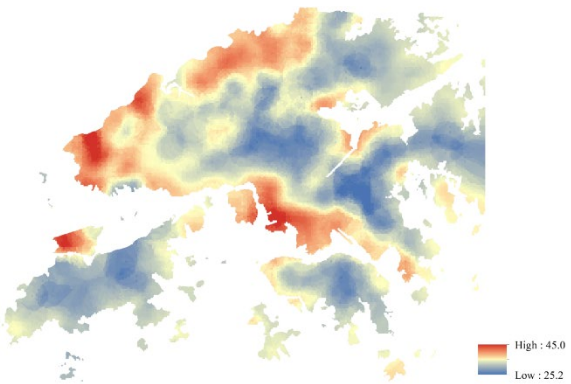

(a3) autumn

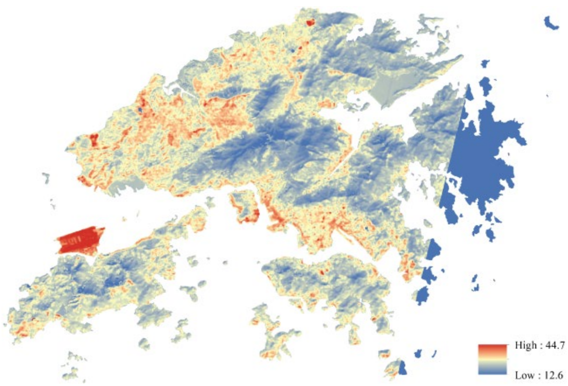

(a4) winter

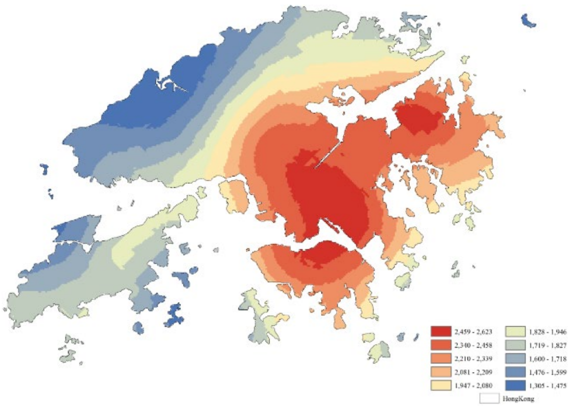

(b)

Fig. 14 Temperature and precipitation indicators of roof greening in Hong Kong. a1-a4, Average temperature by season in 2021. **b**, Precipitation distribution in Hong Kong obtained by data interpolation of 139 stations.

4.4 Priority of roof greening

To judge the urgency of roof greening from the perspective of urban sustainability, we incorporated the six indicators aforementioned and normalized their measurement values, then, assigned equal weights to each indicator to assess the greening priorities (between 0 and 1) of all potential roofs in Hong Kong, while the priorities of roofs unsuitable for greening were set to 0 (Fig. 15).

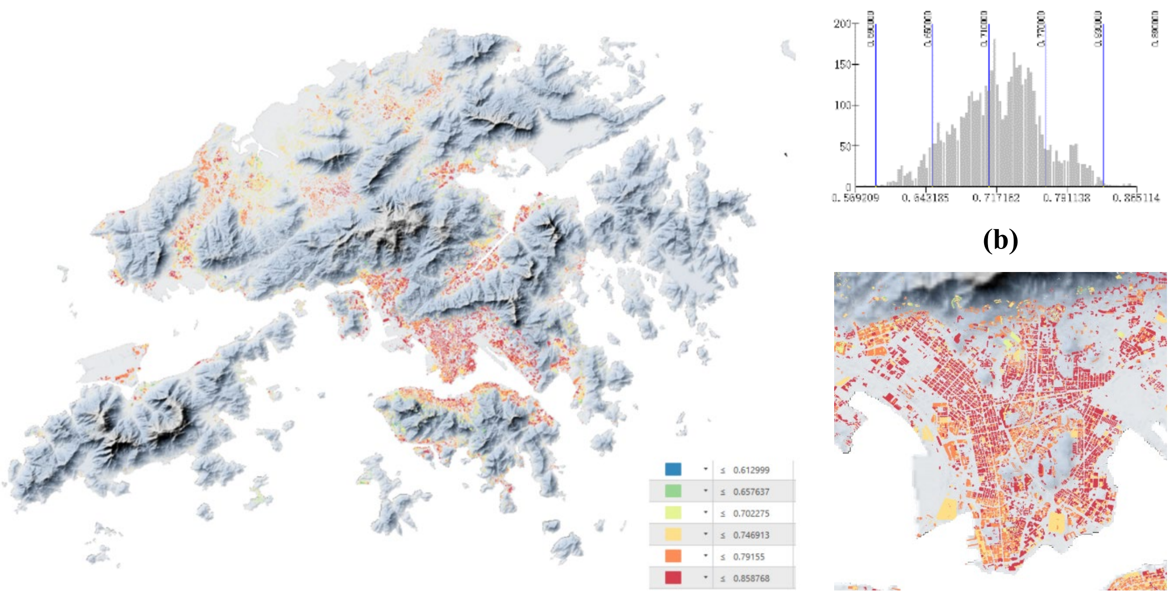

(a) (c)

Fig. 15 Roof greening priority in Hong Kong. **a**, Distribution of greening priority. **b**, Histogram showing the changes of priority values and building numbers. **c**, Examples of roof greening priority in local areas.

Experimental results show that the greening priorities of almost all potential roofs were greater than 0.5, the maximum priority value reached above 0.94, and the average greening priority was about 0.74, which indicated urgent demand for roof greening in Hong Kong. Specifically, the priority of roof greening in urban areas is commonly higher than that in suburban areas. First, the urban areas have low greenspace coverage rate (Fig. 13a), resulting in more needs for greenspaces. Second, due to sparse greenspaces, large amounts of impervious surfaces, and lots of anthropogenic activities, residents in urban areas are exposed to higher thermal stress (Fig. 14a), so demand for heat reduction is greater in urban areas, while suburban areas are less affected by heatwave and have low demand for roof greening, especially in vegetated areas. Third, urban areas generally have more main roads and traffic flows (Fig. 13b), so more greenspaces are needed to reduce the impact of vehicles. On the other hand, the priority of roof greening in built-up areas is generally greater, for example, the average priorities of Kowloon and Hong Kong Island are up to 0.8, while about 0.71 in the New Territories. Although there are more private buildings in Kowloon and Hong Kong Island, which means low priority for the category indicator, they have sparse greenspace areas and complicated main roads due to high-density buildings, moreover, due to different geographical locations, precipitation in Kowloon and Hong Kong Island is greater than that in New Territories. The differences in income and surface temperature between Kowloon and New Territories do not appear to be significant, while a relatively higher income and lower surface temperature appear in Hong Kong Island, meaning lower priority for the two indicators. Accordingly, buildings especially in built-up areas of Kowloon show higher roof greening priorities after incorporating all the indicators.

4.5 Benefits to ecological environment

Hong Kong has a large area of greenspace accounting for about 70% of the land and a low residential land of only 7%. Most greenspaces are woodland and shrubland located in suburbs inaccessible to residents (Tian et al., 2012), while residential land is almost aggregated in urban areas, thereby resulting in a low average greenspace coverage rate around buildings of 0.35 (Fig. 16a), and the rate in urban centers of Kowloon and Hong Kong Island is even less than 0.1 (Fig. 13a). Moreover, due to a high population density in urban areas, human exposure to greenspace index value is only 35.3%, which is far lower than the average level of some developed countries and regions and is in sharp contrast to the high proportion of greenspace in Hong Kong. Whether to change the status quo of uneven greenspaces has become an important issue faced by city planners and public decision-makers. Although roof greening can increase the greenspace area by 63.9 km^2, only about 9% of the existing greenspace area in Hong Kong (Jim & Chan, 2016), it is of great significance to the urban ecological environment. First, green roofs can raise the average greenspace coverage rate around buildings up to 0.58 (Fig. 16b), which greatly improves the greenspace provision in urban areas. Second, human exposure to greenspace index value can be increased to 56.7% and reach a high level globally through roof greening, which not only improves the quality of the ecological environment, but also has the potential to promote the health and well-being of residents. In addition to providing more accessible greenspaces for humans, large-scale green roofs are also expected to contribute to the conservation of urban biodiversity by providing more habitats for other species in Hong Kong.

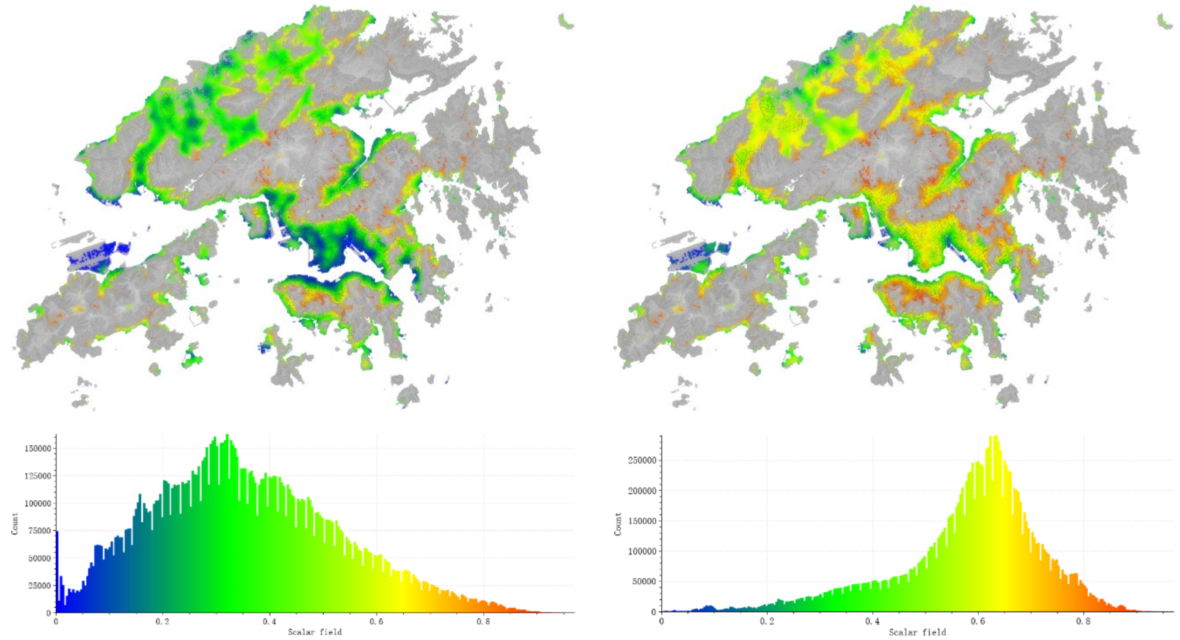

(a) **(b)**

Fig. 16 Greenspace coverage rate around buildings before roof greening (a) and after roof greening (b), the horizontal axis shows the greenspace coverage rate, and the vertical axis shows the count of buildings.

4.6 Urban heat mitigation

Due to the characteristics of geographical location and urbanization, the UHI effect is significant in Hong Kong, so how to mitigate urban heat has become the focus of urban policymakers. Roof greening has been regarded as an effective practice for cooling urban (Wong et al., 2021; He et al., 2020), but it is unclear the effect of mitigating heat across Hong Kong. Therefore, we used Weather Research and Forecasting (WRF)/Urban Canopy Model (UCM) model to simulate the urban heat mitigation effect of the four seasons before and after roof greening (Skamarock et al., 2019). To simplify the simulation process, we selected four representative sunny days, January 15 (winter), April 13 (spring), July 14 (summer), and October 2 (autumn) in 2021. In Fig. 17a, the temperature in urban areas was higher than that in mountainous covered by the dense vegetation, and high-temperature areas in Kowloon and Hong Kong Island were less than that in New Territories due to the evapotranspiration of seawater, which were consistent with the results retrieved from satellite images (Fig. 14a). After roof greening, the air temperature in the territory has dropped from 0-0.4°C, the high-temperature areas have shrunk, and the areas with the largest temperature reduction appeared in the high-density urban areas, especially in New Territories (Fig. 17a). The daily air temperature variation of the four seasons in Hong Kong (Fig. 177b) showed spring was the coldest season with temperatures below 20°C, so no need for cooling; the air temperatures were high in summer and autumn, resulting in an urgent need for cooling. The air temperature in winter is kept at a relatively high level, but the need for cooling is low. Additionally, the peak air temperature reduction was recorded between 13:00 and 16:00 p.m., during which time the ground radiation was the strongest, and the evaporation from porous surfaces would be more, so more temperature reduction. Due to surface heat loss and less evaporation, the cooling effect of green roofs was worst around 8:00 a.m., and there is even a warming effect in other seasons except for autumn (Fig. 17b). Overall, the results indicated the cooling potential of green roofs in Hong Kong.

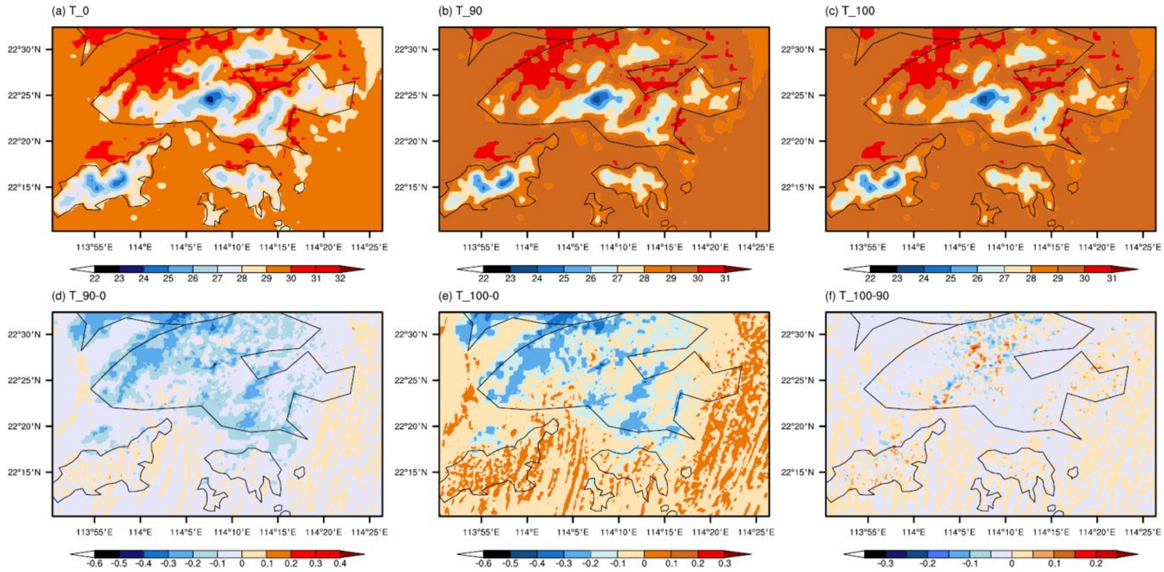

(a)

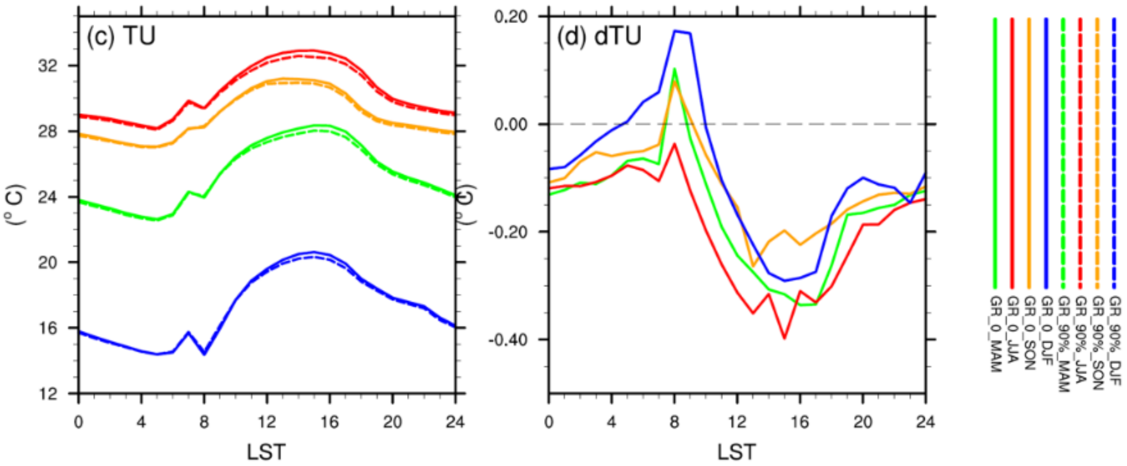

(b)

Fig. 17 Air temperature simulation of four seasons in Hong Kong. a, The distribution of air temperature before and after roof greening. **b**, Simulating daily air temperature variation before and after roof greening and air temperature reduction through roof greening.

4.7 Carbon emission reduction

In the process of urbanization, increased anthropogenic activity, such as burning coal, natural gas, and oil, is increasing the emission of carbon dioxide, leading to climate change and global warming. To stem the climate crisis, countries pledged in the 2015 Paris Agreement to achieve net-zero emissions by 2050 or earlier. In line with the agreement, the Chinese government set a carbon neutrality development goal, which aims to offset carbon dioxide through some ways, such as afforestation, energy conservation, and pollution reduction, to achieve relatively zero emissions. Green roofs are roofs covered with different kinds of vegetation and growing substrate (Shafique et al., 2018), which can increase carbon stocks and benefit carbon sequestration. We estimated that 63.9 km^2 of potential green roofs can increase about 820,000 metric tons of carbon stocks in Hong Kong, where the vegetation and soil provide about 40,000 and 780,000 metric tons, respectively. Furthermore, green roofs can reduce carbon emissions in two patterns. First, the carbon can be captured by vegetation through photosynthesis as well as stored by the soil, and the carbon storage potential of green roofs is about 10 $\mathrm{kg} \cdot (\mathrm{m}^2 \cdot \mathrm{a})^{-1}$. Thus, 63.9 km^2 of green roofs could reduce about 640,000 metric tons of carbon emissions in one year. Indirectly reducing carbon emissions through energy saving is another pattern. We estimated that the pattern could reduce carbon emissions by about 370,000 metric tons in one year. Accordingly, the annual equivalent of carbon emissions reduced by green roofs is about 1,010,000 metric tons, which can offset about 3% of annual carbon emissions in Kong Hong. This indicates that more than just green roofs are needed to realize Hong Kong's carbon-neutral goal.

4.8 Benefits to social economy

Currently, there is still a lack of direct evaluation of the social economic benefits of green roofs, which has restricted the decision-making process of roof greening (Teotónio et al., 2021). In general, the economic benefits of green roofs were evaluated indirectly from the aspects of energy saving and carbon pricing. Energy saving is reflected in urban heat mitigation, that is, green roofs could save electricity energy for building cooling by reducing the air temperature. Given the climatic characteristics, assuming the time period for cooling is throughout summer and autumn, and extensive green roof is a dominant type, then the electricity energy can be saved by about 4.68×10^8 $\mathrm{kW} \cdot \mathrm{h}$. Translated into monetary units, the total electricity energy cost saving is about HK\$ 603.7 million with an electricity tariff at the site of $1.29\ \mathrm{HK\$} \cdot (\mathrm{kW} \cdot \mathrm{h})^{-1}$ unit in 2023. On the other hand, with the promotion of carbon neutral goals, carbon trading provides a low-cost and strong incentive scheme for global carbon emission reduction, and the trading system has gradually been established and improved. Taking the transaction price (about $65\ \mathrm{HK\$} \cdot \mathrm{t}^{-1}$) of China's carbon market in June 2023 as a reference, the monetary values of carbon emission reduction benefits are about HK\$ 65.7 million in one year. Overall, green roofs could bring a total annual value of around HK\$ 669.4 million.

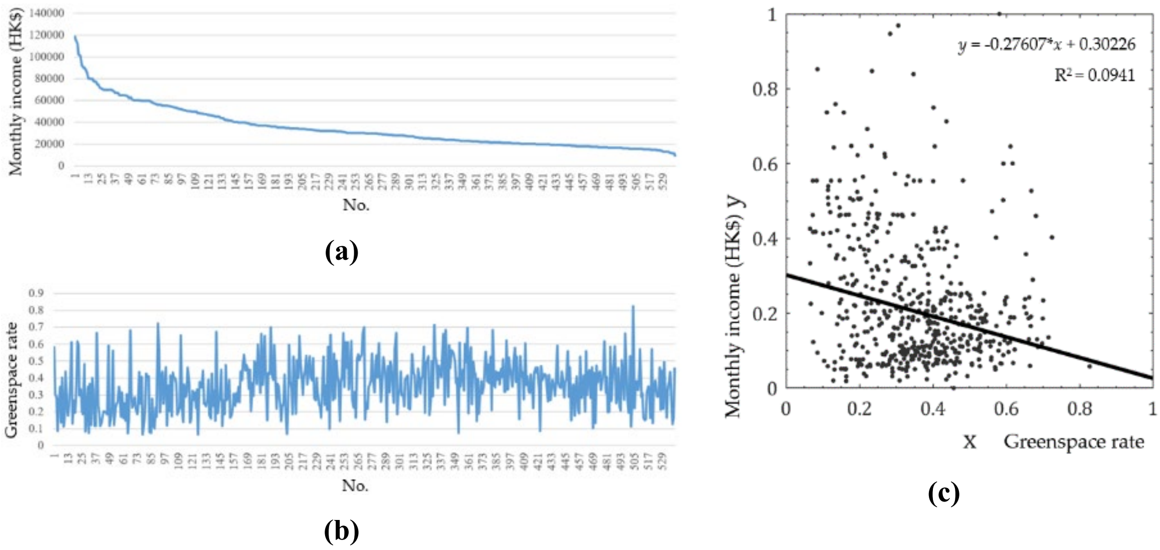

Fig. 18 Correlation (c) between monthly income (a) and greenspace rate (b) of buildings. a, The income data comes from the monthly median income of 540 housing estates in 2021 according to Hong Kong government statistics. **b**, Greenspace coverage rate indicates the proportion of greenspace area within the 500-meter neighbourhood of the building.

Moreover, the relationship between greenspaces and humans is a topic gotten more attention in the field of social economics, many researchers have explored the differences in access to greenspace services of different socioeconomic classes (Chiang & Li, 2019; Greene et al., 2018). Some studies have found inequality in the access to greenspaces of resident groups, while the inequality runs counter to the goal of social justice in sustainable development. For example, most researchers represented that the advantaged residents (such as high income and high education) tend to enjoy more abundant greenspaces (Ferguson et al., 2018; Yin et al., 2023), while some researchers have taken contradictory conclusions from their study areas (Liu et al., 2017; Xiao et al., 2017). Overall, these findings have implications for assessing green roofs. To assess the socioeconomic benefit in Hong Kong, thus, we analyzed the correlation between the monthly income and the greenspace coverage rate. Fig. 18a showed a vast difference in the median monthly income of different groups, with the richest earning ten times more than the poorest. On the contrary, the overall greenspace coverage rate (Fig. 18b) of the 540 housing estates was relatively equal. As a result, we observed a significant weak negative correlation between the median monthly income and the greenspace coverage rate ($r = -0.31, P < 0.01$; Fig. 18c), which indicates different groups have considerable fairness in enjoying greenspace services, but indirectly suggests that green roofs have a limited impact on the social economic benefit of increasing monthly median income in Hong Kong.

5. Policy Implications and Recommendations

Hong Kong is committed to building a sustainable city with low-carbon and smart characteristics, ensuring that future generations can continue to thrive in a livable and green environment. The HK government is striving to uplift the quality of living environment through planting and preservation of vegetation. The target is to give rise to notable improvements in urban greenery by enhancing existing greened areas and opportunities of quality greening during urban planning and development. The environmental, social and ecological contributions of green roofs to creating sustainable living in high-density cities are accepted worldwide (Hong et al., 2019; Manso et al., 2021), since it is possible to incorporate the concept of green roofs into the landscape design and urban planning, hence reducing the environmental impacts and improving the quality of life.

According to the published Smart City Blueprint for Hong Kong 2017 and Hong Kong's Climate Action Plan 2030+, the city intends to become a low carbon, climate resilient and smart greening city. Hong Kong strives to achieve carbon neutrality before 2050 and will reduce its carbon intensity by 65% by 2030 in order to meet the Paris Agreement's goal <=1.5°C-2°C with the help of developing smart city geospatial techniques at the same time. New technology and applications need to be developed to boost carbon neutralization investments conducive to reducing carbon emissions and build a low-carbon economy which is more resilient to climate change. For example, the Council for Sustainable Development of the HK government reviewed the policy of allowing buildings to develop rooftop areas to include greenness for enhancing the livelihood quality (Shafique & Luo, 2019). The package strikes a proper balance between fulfilling environment performance and comfort requirements of buildings while minimizing the impact on the surroundings. However, to achieve the policy targets, more efforts are needed to determine suitable technologies and policy for promoting the green roof system. Government needs to develop strategies aiming to encourage both private sector and community participation (Tan et al., 2021). The main initiatives being undertaken include active planning program, enhancing opportunities of quality greening, and community support with private sector involvement. The objective of the project is to conduct a study of identifying potential locations for GRs deployment in Hong Kong using latest geospatial intelligence approaches, and to recommend guidelines based on the quantified benefits to adaptively address local demands and priority to promote public understandings and awareness.

According to project research and experimental results, we have the following suggestions about roof greening for city planners and policy makers:

1. Identification of green roofs: 3D Geometry and load bearing are two important factors to be considered for selection of green roofs. In the aspect of 3D geometry, a roof with an area of more than 10 m^2 and a slope less than 15 degrees is suggested suitable for greening retrofit. In the aspect of load bearing, building age can be used to judge whether the roof can be greened, in which a building less than 50 years old can be considered sufficient in load-bearing capacity to host greenery on the roof.

2. Evaluation of roof greening priority: Indicators of environment, social economy, and climate, which are closely related to urban sustainable development and human well-being, are suggested to evaluate the priority of roof greening. Greenspace coverage around buildings and the nearest distance between the building and the main transportation networks can be considered to quantify the environmental indicator. Building categories (including private, public, and miscellaneous) and resident's monthly income can be used to quantify the social economy indicator. The mean surface temperature in different seasons and annual precipitation can be used to quantify the climate indicator. Given the equal importance of all indicators in urban sustainability, equal weight is suggested to be given to these indicators for evaluating roof greening priority. The policy maker can also adapt the weighting factors in order to adjust and meet the priority goals according to new requirements or criterion.

3. 63.9 km^2 of building roofs can be green retrofitted, accounting for around 90% of the total roof area (70.1 km^2) in Hong Kong. Greening priorities of almost all potential roofs are greater than 0.5, the maximum priority value reaches above 0.94, and the average greening priority is about 0.74, in which nearly 80% (51.12 km^2) of potential green roofs have a priority of 0.7 or higher. In Kowloon, especially Sham Shui Po and Kwun Tong districts, the roof greening priorities are the two highest in Hong Kong. Additionally, the greening priorities of building roofs in urban areas are generally greater than those in suburban areas.

4. First, potential green roofs can increase the greenspace area by 63.9 km^2, which can raise the average greenspace coverage rate around buildings from 0.35 to 0.58 and can increase human exposure to greenspace index value from 35.3% to 56.7%. This greatly improves the greenspace provision in urban areas, meanwhile, large-scale green roofs are also

expected to contribute to the conservation of urban biodiversity by providing more habitats for other species in Hong Kong. Second, according to roof greening, the air temperature in the territory can drop by from 0-0.4℃, and the high-temperature areas also can shrink, in which the areas with the largest temperature reduction appear in the high-density urban areas, especially in New Territories. Next, 63.9 km^2 of potential green roofs can increase by about 820,000 metric tons of carbon stocks in Hong Kong and could reduce/offset carbon emissions by about 640,000 metric tons through photosynthesis and about 370,000 metric tons through soil storage in one year. Accordingly, the annual equivalent of carbon emissions reduced by green roofs is about 1,010,000 metric tons, which is equivalent to offsetting about 3% of annual carbon emissions in Kong Hong. In the aspect of social economy, green roofs can save electricity energy by about 4.68×10^8 kW · h, the total electricity energy cost saving is about HK$ 603.7 million in 2023, meanwhile, the monetary values of carbon emission reduction benefits are about HK$ 65.7 million in one year. Overall, green roofs could bring a total annual value of around HK$ 669.4 million.

6. Details of the Public Dissemination held

6.1 Research Paper

On top of research activities findings, the research team also planned to publish research articles in peer-review journals. Given the relatively short research period, the team will focus more on publication after the submission of the research report and is going to submit at least one academic article within 2023. Based on the findings of this research project, a research paper is submitted to the Journal of Nature Sustainability. It is temporarily titled as "Prioritizing green roofs for supporting urban sustainability in Hong Kong". This paper aims at conveying the novel formation of roof greening and introducing the impact of prioritized urban roof greening on the Hong Kong situation to the Geospatial and urban sustainability community.

6.2 International Conference

We presented the preliminary findings of this research at ISPRS XXIV General Congress. It is an academic conference held on 6^{th}-11^{th} June 2022, focusing on photogrammetry and remote sensing. In particular, the research team presented this research project in terms of the building reconstruction methodologies and results in the title of "Extraction of Orthogonal Building Boundary from Airborne LIDAR Data Based on Feature Dimension Reduction", explained how the cutting-edge geospatial intelligence technology achieved the research findings, and the research's implication to Hong Kong's urban building modelling and construction. The research team is open to join more academic conferences in the coming future.

An international Conference, "The ISPRS Workshop on GEOAI for SDGs,", was held on July. 02-07, 2023. The PI and research team presented this research project in terms of the project scope, methodologies and research findings in the title of "Priority analysis and evaluation of building roof greening in HK". This conference was participated with academics in the aspects of geospatial, remote sensing, urban science, computer science etc.

An international Conference, "The 2023 Asian Conference on Remote Sensing (ACRS2023)", will be held on Oct.30 - Nov.3, 2023. The PI and research team has submitted an abstract and will present this research project in terms of the project scope, methodologies and research findings in the title of "The Evaluation of Roof Greening priority and benefits in Hong Kong". This conference will be participated with academics in the aspects of geospatial, remote sensing science, geo/earth-science computer science etc. Meanwhile, The PI and research team has also submitted another abstract and will present the research project in terms of the building roof extraction methodologies and research findings with the title of "Fine-grained Classification of Urban Buildings using Low-resolution Overhead Images", which is also one of major research outcomes and merits of this project.

6.3 Public Dissemination

After the completion of the project, the research team plans to hold a seminar to disseminate the findings of this research and collect initial feedback from related professionals to help strengthen potential usability of the research findings. We hope to invite policymaker, such as Planning Department, the Innovation, Technology and Industry Bureau; and representatives from relevant professional organizations, like the Hong Kong, the Hong Kong Association for Surveying (HKIS), International Society for Urban Informatics (ISUI) and the IEEE Geoscience and Society Hong Kong Chapter. Media, academics, teachers, students and the general public are also welcomed to join.

7. Conclusions

Greenspaces are pieces of urban nature designed to reduce the negative effects of urbanization and protect people's health, particularly providing universal access to greenspaces has become one of the targets of Sustainable Development Goal 11 "Sustainable cities and communities". Green roofs have the potential to provide additional greenspaces and have been regarded as an effective strategy to mitigate the adverse impacts of urbanization. Hong Kong is a thoroughly urbanized city with a dense population and uneven greenspace in build-up areas and is in the subtropical region, where high-density buildings and impervious surfaces lead to distinct urban heat island effects and intensive anthropogenic activities have increased carbon emissions. As a result, urban sustainability faces serious challenges in Hong Kong. To address the challenge, we used geospatial big data to comprehensively assess the priority and benefits of green roofs from the perspective of urban sustainability at the urban scale and overcome the limitation of separate evaluation of small-scale green roofs based on limited data and indicators, thereby enhancing the cognition of green roofs. Specifically, building geometry and attribute information were used to identify the potential roofs; different from the indicators based on only attributes, we focused on several indicators closely related to urban sustainability and quantified them to determine the urgency of roof greening under different conditions, then combined all indicators to assess the greening priority and benefits of all potential roofs.

Through a multifaceted assessment, we found the area of the potential roofs that can be greened reaches about 90% in Hong Kong and most potential roofs show the urgent need for greening, where the average greening priority was 0.74 and the greening priority of ~81% of the potential roofs up to 0.7, especially in urban cores. Additionally, we estimated that green roofs can increase the greenspace coverage rate around buildings from 0.35 to 0.58 and human exposure to greenspace from 35.3% to 56.7%, which could reach a high level globally; temperature simulation results showed that green roofs can reduce the air temperature by 0-0.4℃; we also estimated that green roofs can provide 820,000 metric tons of additional carbon storage and have the potential to offset ~3% of annual carbon emissions in Hong Kong, and at the same time, bring hundreds of millions (HK$) in economic performance a year. Our explicit insights can support prioritizing greening policies and sustainable development in Hong Kong and other cities across the globe.

8. Main References

Aboelata, A. (2021). Assessment of green roof benefits on buildings' energy-saving by cooling outdoor spaces in different urban densities in arid cities. Energy, 219, 119514.

Chen, B., Wu, S., Song, Y., Webster, C., Xu, B., Gong, P. (2022). Contrasting inequality in human exposure to greenspace between cities of Global North and Global South. Nature Communications 13, 4636.

Chiang, Y. C. & Li, D. (2019). Metric or topological proximity? The associations among proximity to parks, the frequency of residents' visits to parks, and perceived stress. Urban Forestry & Urban Greening 38, 205-214.

Demographia. (2022). Demographia world urban areas 18th annual editor: 202207.

Dizdaroglu, D., Yigitcanlar, T., & Dawes, L. (2012). A micro-level indexing model for assessing urban ecosystem sustainability. Smart Sustain. Built Environ., 1(3), 291–315.

Dorst, H., van der Jagt, A., Raven, R., & Runhaar, H. (2019). Urban greening through nature-based solutions – Key characteristics of an emerging concept. Sustain. Cities Soc., Vol. 49, p. 101620.

Ferguson, M., Roberts, H. E., McEachan, R. R. C., Dallimer, M. (2018). Contrasting distributions of urban green infrastructure across social and ethno-racial groups. Landscape and Urban Planning 175, 136-148.

Gou, Z., Xie, X., Lu, Y., & Khoshbakht, M. (2018). Quality of Life (QoL) survey in Hong Kong: Understanding the importance of housing environment and needs of residents from different housing sectors. International journal of environmental research and public health, 15(2), 219.

Grandvalet, Y., Bengio, Y. (2004). Semi-supervised learning by entropy minimization. In: Proceedings of the 17th International Conference on Neural Information Processing Systems, p. 529–536.

Greening Hong Kong. https://www.gov.hk/en/residents/environment/sustainable/greening.htm

Greene, C. S., Robinson, P. J. & Millward, A. A. (2018). Canopy of advantage: who benefits most from city trees? Journal of Environmental Management 208, 24-35.

Grunwald, L., Heusinger, J., & Weber, S. (2017). A GIS-based mapping methodology of urban green roof ecosystem services applied to a Central European city. Urban Forestry & Urban Greening, 22, 54-63.

He, Y., Yu, H., Ozaka, A., Dong, N. (2020). Thermal and energy performance of green roof and cool roof: A comparison study in Shanghai area. Journal of Cleaner Production 267, 122205.

Herrera-Gomez, S. S., Quevedo-Nolasco, A., & Pérez-Urrestarazu, L. (2017). The role of green roofs in climate change mitigation. A case study in Seville (Spain). Building and Environment, 123, 575-584.

Ho, J., Jain, A., Abbeel, P. (2020). Denoising diffusion probabilistic models, in: Advances in Neural Information Processing Systems (NeurIPS), Curran Associates, Inc.. pp. 6840-6851.

Hoeben, A. D., & Posch, A. (2021). Green roof ecosystem services in various urban development types: A case study in Graz, Austria. Urban Forestry & Urban Greening, 127167.

Hong, W., Guo, R. &Tang, H. (2019). Potential assessment and implementation strategy for roof greening in highly urbanized areas: A case study in Shenzhen, China. Cities, 95, 102468.

Goodfellow, I. J., Pouget-Abadie, J., Mirza, M., Xu, B., Warde-Farley, D., Ozair, S., Courville, A., & Bengio, Y. (2014). Generative Adversarial Networks. NIPS.

Iscen, A., Tolias, G., Avrithis, Y., Chum, O. (2019). Label propagation for deep semi-supervised learning. In: 2019 IEEE/CVF Conference on Computer Vision and Pattern Recognition (CVPR), pp. 5065–5074.

Jim, C. Y. & Chan, M. W. H. (2016). Urban greenspace delivery in Hong Kong: spatial-institutional limitations and solutions. Urban Forestry & Urban Greening 18, 65-85.

Joshi, M. Y., Selmi, W., Binard, M., Nys, G.-A., and Teller, J. (2020). Potential for urban greening with green roofs: A way towards smart cities, ISPRS Ann. Photogramm. Remote Sens. Spatial Inf. Sci., VI-4/W2-2020, 87–94.

Karras, T., Aila, T., Laine, S., & Lehtinen, J. (2018). Progressive growing of gans for improved quality, stability, and variation. In ICLR, 2018.

Laine, S., Aila, T. (2017). Temporal ensembling for semi-supervised learning. In: 5th International Conference on Learning Representations, ICLR 2017.

Langemeyer, J., Wedgwood, D., McPhearson, T., Baró, F., Madsen, A. L., & Barton, D. N. (2020). Creating urban green infrastructure where it is needed – A spatial ecosystem service-based decision analysis of green roofs in Barcelona. Sci. Total Environ., 707, 135487.

Lee, L. S., & Jim, C. Y. (2018). Thermal-cooling performance of subtropical green roof with deep substrate and woodland vegetation. Ecological Engineering, 119, 8-18.

Levin, D. (2004). Mesh-independent surface interpolation, G. Brunnett, B. Hamann, H. Müller, L. Linsen (Eds.), Geometric Modeling for Scientific Visualization, Springer, Berlin Heidelberg, Berlin Heidelberg (2004), pp. 37-49.

Liu, W. P., Chen, W. J. & Dong, C. L. (2017). Spatial decay of recreational services of urban parks: characteristics and influencing factors. Urban Forestry & Urban Greening 25, 130-138.

Mallinis, G., Karteris, M., Theodoridou, I., Tsioukas, V., & Karteris, M. (2014). Development of a nationwide approach for large scale estimation of green roof retrofitting areas and roof-top solar energy potential using VHR natural colour orthoimagery and DSM data over Thessaloniki, Greece. Remote Sens. Lett., 5(6), 548–557.

Manso, M., Teotónio, I., Silva, C. M., & Cruz, C. O. (2021). Green roof and green wall benefits and costs: A review of the quantitative evidence. Renewable and Sustainable Energy Reviews, 135, 110111.

Oehrlein, J., Niedermann, B., & Haunert, J. H. (2019). Analyzing the Supply and Detecting Spatial Patterns of Urban Green Spaces via Optimization. J. Photogramm. Remote Sens. Geoinf. Sci., 87(4), 137–158.

Peng, L. L. H., & Jim, C. Y. (2015). Economic evaluation of green-roof environmental benefits in the context of climate change: The case of Hong Kong. Urban For. Urban Green., 14(3), 554–561.

Rabbani, T., Van Den Heuvel, F., & Vosselmann, G. (2006). Segmentation of point clouds using smoothness constraint. International archives of photogrammetry, remote sensing and spatial information sciences, 36(5), 248-253.

Santos, T., Tenedório, J. A., & Gonçalves, J. A. (2016). Quantifying the city's green area potential gain using remote sensing data. Sustainability, 8(12), 1247.

Shafique, M., & Luo, X. (2019). Green roofs as an effective strategy for the reduction of CO2 emission: A review. Paper presented at CIB World Building Congress 2019 (CIB WBC 2019) "Constructing Smart Cities", Hong Kong, Hong Kong.

Shafique, M., Kim, R., & Rafiq, M. (2018). Green roof benefits, opportunities and challenges – A review. Renew. Sustain. Energy Rev., Vol. 90, pp. 757–773.

Shafique, M., Azam, A., Rafiq, M., Ateeq, M., Luo, X. (2020). An overview of life cycle assessment of green roofs. Journal of Cleaner Production 250, 119471.

Shao, J., Zhang, W., Shen, A., Mellado, N., Cai, S., Luo, L., Wang, N., Yan, G., Zhou, G. (2021). Seed point set-based building roof extraction from airborne LiDAR point clouds using a top-down strategy. Automation in Construction 126, 103660.

Shannon, C.E. (1948). A mathematical theory of communication. Bell Syst. Tech. J. 27, 379–423.

Sharma, A., Woodruff, S., Budhathoki, M., Hamlet, A. F., Chen, F., & Fernando, H. J. S. (2018). Role of green roofs in reducing heat stress in vulnerable urban communities - A multidisciplinary approach. Environ. Res. Lett., 13(9).

Silva, C. M., Flores-Colen, I., Antunes, M. (2017). Step-by-step approach to ranking green roof retrofit potential in urban areas: A case study of Lisbon, Portugal. Urban Forestry & Urban Greening 25, 120-129.

Skamarock, W. C., Klemp, J. B., Dudhia, J., Gill, D. O., Liu, Z., Berner, J., … Huang, X. -yu. (2019). A Description of the Advanced Research WRF Model Version 4.1 (No. NCAR/TN-556+STR).

Sodiq, A., Baloch, A. A. B., Khan, S. A., Sezer, N., Mahmoud, S., Jama, M., & Abdelaal, A. (2019). Towards modern sustainable cities: Review of sustainability principles and trends. J. Clean. Prod., Vol. 227, pp. 972–1001.

Sohl-Dickstein, J., Weiss, E., Maheswaranathan, N., Ganguli, S. (2015). Deep unsupervised learning using nonequilibrium thermodynamics, in: Proceedings of the 32nd International Conference on Machine Learning (ICML), pp. 2256–2265.

Song, Y., Chen, B., Ho, H.C., Kwan, M.P., Liu, D., Wang, F., Wang, J., Cai, J., Li, X., Xu, Y., He, Q., Wang, H., Xu, Q., Song, Y.Z. (2021). Observed inequality in urban greenspace exposure in China. Environmental International 156, 106778.

Stephenne, N., Beaumont, B., Hallot, E., Wolff, E., Poelmans, L., & Baltus, C. (2016). Sustainable and smart city planning using spatial data in Wallonia. ISPRS Ann. Photogramm. Remote Sens. Spat. Inf. Sci., IV-4/W1, 3–10.

STUDY ON GREEN ROOF APPLICATION IN HONG KONG, ARCHITECTURAL SERVICES DEPARTMENT (2007). https://www.archsd.gov.hk/media/studies-and-report/study-on-green-roof-applications-in-hong-kong-final-report-by-architectural-service-department/green_roof_study_final_report.pdf

Tagaris, T., Sdraka, M., & Stafylopatis, A. (2019). High-resolution class activation mapping. In 2019 IEEE international conference on image processing (ICIP) (pp. 4514-4518).

Tan, Y., Luo, T., Xue, X., Shen, G. Q., Zhang, G., & Hou, L. (2021). An empirical study of green retrofit technologies and policies for aged residential buildings in Hong Kong. Journal of Building Engineering, 39, 102271.

Tarvainen, A., Valpola, H. (2017). Mean teachers are better role models: Weight-averaged consistency targets improve semi-supervised deep learning results. In: Advances in Neural Information Processing Systems, pp. 1195–1204.

Teotónio, I., Silva, C. M. & Cruz, C. O. (2021). Economics of green roofs and green walls: a literature review. Sustainable Cities and Society 69, 102781.

Thomas, H., Qi, C.R., Deschaud, J.E., Marcotegui, B., Goulette, F., Guibas, L. (2019). Kpconv: Flexible and deformable convolution for point clouds. In: 2019 IEEE/CVF International Conference on Computer Vision (ICCV), pp. 6410–6419.

Tian, Y., Jim, C. Y. & Tao, Y. (2012). Challenges and strategies for greening the compact city of Hong Kong. Landscape and Urban Planning 158, 101-109.

UN-Habitat. (2012). State of the world's cities 2012/2013: Prosperity of cities. Nairobi, Kenya: UN-Habitat.

Wang, P., & Yao, W. (2022). A new weakly supervised approach for ALS point cloud semantic segmentation. ISPRS Journal of Photogrammetry and Remote Sensing, 188, 237-254.

Wong, N. H., Tan, C., Kolokosta, D.D., Takebayashi, H. (2021). Greenery as a mitigation and adaptation strategy to urban heat. Nature Reviews Earth & Environment 2, 166-181.

Wong, P. W. C., Yu, R. W. M., Ngai, J. T. K. (2019). Companion animal ownership and human well-being in a metropolis – the case of Hong Kong. International Journal of Environmental Research and Public Health 16, 1729.

Wonho, B., Noh, J., & Kim, G. (2020). Rethinking class activation mapping for weakly supervised object localization. Computer Vision–ECCV 2020: 16th European Conference, Glasgow, UK, August 23–28, 2020, Proceedings, Part XV 16. Springer International Publishing.

Wu, Y., Zhang, W., Shen, J., Mo, Z., & Peng, Y. (2018). Smart city with Chinese characteristics against the background of big data: Idea, action and risk. J. Clean. Prod., 173, 60–66.

Xiao, Y., Wang, Z., Li, Z., Tang, Z. (2017). An assessment of urban park access in Shanghai: implications for the social equity in urban China. Landscape and Urban Planning 157, 383-393.

Xu, Y., Wu, S., Guo, M., Xie, X. (2021). A framework for the evaluation of roof greening priority. Building and Environment 206, 108392.

Yao, W., & Wei, Y. (2013). Detection of 3-D individual trees in urban areas by combining airborne LiDAR data and imagery. IEEE Geoscience and Remote Sensing Letters, 10(6), 1355-1359.

Yin, Y., He, L., Wennberg, P., Frankenberg, C. (2023). Unequal exposure to heatwaves in Los Angeles: impact of uneven green spaces. Science Advances 9, eade8501.